AD-A065 857 FOREIGN TECHNOLOGY DIV WRIGHT-PATTERSON AFB OHIO F/G 17/9
THEORETICAL PRINCIPLES OF RADAR (CHAPTER 7, 7.1 - 7.16),(U)
SEP 78 Y D SHIRMAN

UNCLASSIFIED FTD-ID(RS)T-1338-78 NL

1 OF 2
AD A
065857

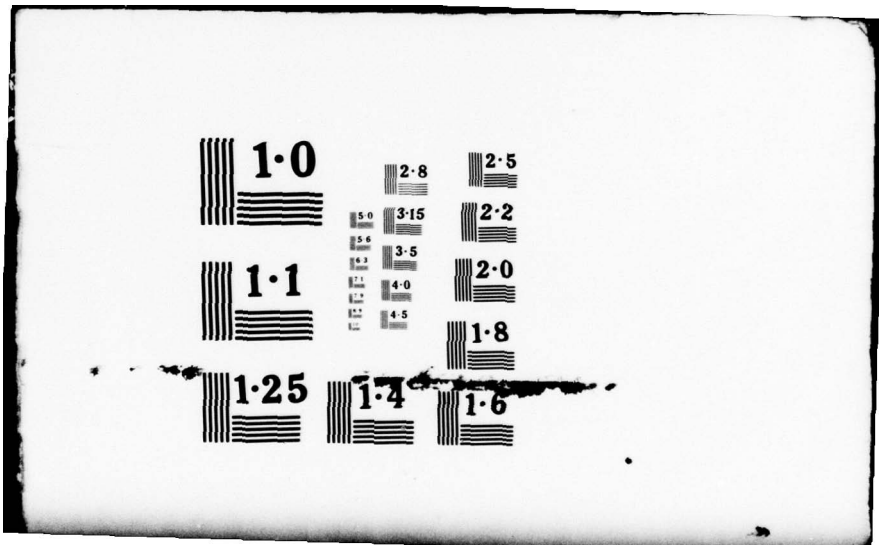
1·0
1·1
1·25
1·4
1·6
1·8
2·0
2·2
2·5
2·8
3·15
3·5
4·0
4·5
5·0
5·6

FTD-ID(RS)T-1338-78

0

# FOREIGN TECHNOLOGY DIVISION


THEORETICAL PRINCIPLES OF RADAR
(CHAPTER 7, §7.1-§7.16)

By

Ya. D. Shirman

# UNEDITED MACHINE TRANSLATION

FTD-ID(RS)T-1338-78 28 September 1978

MICROFICHE NR: FTD-78-C-001328

THEORETICAL PRINCIPLES OF RADAR (CHAPTER 7, §7.1-§7.16)

By: Ya. D. Shirman

English pages: 133

Source: Teoreticheskiye Osnovy Radiolokatsii, Izd-vo "Sovetskoye Radio," Moscow, 1970, pp. 421-479.

Country of origin: USSR
This document is a machine translation.
Requester: FTD/PHE
Approved for public release; distribution unlimited.

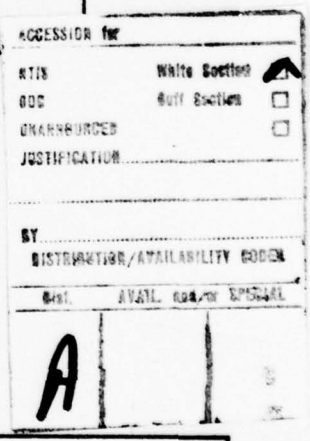




PREPARED BY:

TRANSLATION DIVISION
FOREIGN TECHNOLOGY DIVISION
WP-AFB, OHIO.

Table of Contents

## U. S. BOARD ON GEOGRAPHIC NAMES TRANSLITERATION SYSTEM

| Block | Italic | Transliteration | Block | Italic | Transliteration |
|---|---|---|---|---|---|
| А а | *А а* | A, a | Р р | *Р р* | R, r |
| Б б | *Б б* | B, b | С с | *С с* | S, s |
| В в | *В в* | V, v | Т т | *Т т* | T, t |
| Г г | *Г г* | G, g | У у | *У у* | U, u |
| Д д | *Д д* | D, d | Ф ф | *Ф ф* | F, f |
| Е е | *Е е* | Ye, ye; E, e* | Х х | *Х х* | Kh, kh |
| Ж ж | *Ж ж* | Zh, zh | Ц ц | *Ц ц* | Ts, ts |
| З з | *З з* | Z, z | Ч ч | *Ч ч* | Ch, ch |
| И и | *И и* | I, i | Ш ш | *Ш ш* | Sh, sh |
| Й й | *Й й* | Y, y | Щ щ | *Щ щ* | Shch, shch |
| К к | *К к* | K, k | Ъ ъ | *Ъ ъ* | " |
| Л л | *Л л* | L, l | Ы ы | *Ы ы* | Y, y |
| М м | *М м* | M, m | Ь ь | *Ь ь* | ' |
| Н н | *Н н* | N, n | Э э | *Э э* | E, e |
| О о | *О о* | O, o | Ю ю | *Ю ю* | Yu, yu |
| П п | *П п* | P, p | Я я | *Я я* | Ya, ya |

*ye initially, after vowels, and after ъ, ь; e elsewhere.
When written as ё in Russian, transliterate as yё or ё.

## RUSSIAN AND ENGLISH TRIGONOMETRIC FUNCTIONS

| Russian | English | Russian | English | Russian | English |
|---|---|---|---|---|---|
| sin | sin | sh | sinh | arc sh | $\sinh^{-1}$ |
| cos | cos | ch | cosh | arc ch | $\cosh^{-1}$ |
| tg | tan | th | tanh | arc th | $\tanh^{-1}$ |
| ctg | cot | cth | coth | arc cth | $\coth^{-1}$ |
| sec | sec | sch | sech | arc sch | $\operatorname{sech}^{-1}$ |
| cosec | csc | csch | csch | arc csch | $\operatorname{csch}^{-1}$ |

| Russian | English |
|---|---|
| rot | curl |
| lg | log |

Page 421.

Chapter 7.

# FUNDAMENTAL FORMS OF INTERFERENCES WITH ACTIVE RADAR AND THE PRINCIPLES OF INTERFERENCE ELIMINATION.

## §7.1. Fundamental forms of interferences with active radar.

As in broadcasting, radio communication and television, in radar can substantially manifest itself the effect of the various kinds of interferences. Rolle these interferences in active radar can prove to be still greater than in other branches of radic engineering, since usually occurs the essertial weakening cf signal on the path of propagation to target/purpose and vice versa. Furthermore, in radar considerably more important role play some specific forms of the interferences with which much more rarely it is necessary to be counted, for example in radio communication. Such interferences are in particular, passive jamming, caused by re-reflection from interfering objects. Together with them in a number of cases,

substantially manifest themselves the active jamming, caused of various kinds by radiation sources.

On their origin of interference, they can be natural, linked and artificial.

Natural ones are the interferences of natural origin. For example, natural passive interferences are formed via re-reflection from hills, mountains, clouds, etc. The natural active jamming (see §5.8) they are created by the radiations of the Sun and other extraterrestrial sources. The active jamming, produced by the effect of the emission/radiations of different radio-electronic means on each other, call linked interferences. Together with linked active jamming are sometimes observed also the mutual passive interferences when in mountainous country interference with radar is created because of the re-reflection of the oscillation/vibrations, emitted by another radar.

Artificial active and passive interferences were placed to radars of military designation/purpose during combat operations in the course of the Second World War, wars in Korea, in the Near East and in Vietnam. According to the published data on military doctrine of the USA, the creation of interferences is one of the forms of electronic warfare. Under electronic war in the USA, understand the

goal-directed preparation and conducting military actions, considering wide use radio electronics in the military technique of enemy.

Page 422.

According to the character of the effect of interference, are divided into masking and simulating. Masking interferences create the background against which difficult to isolate the signal, covered by interference; at the same time they usually victim signal in the nonlinear cell/elements of receiver. The imitative interferences create the effect of confusing reflectors, impeding obtaining information about true target/purposes. Each of three the varieties indicated above of interferences (natural, mutual and man-made interference) can be in turn, masking or simulating.

The examination of interferences and principles of protection from them is expedient to begin from the masking interferences. The masking active and passive interferences (natural, reciprocal, artificial) and the possible principles of protection from them will be examined. Then a similar examination is briefly conducted for the simulating interferences. On intra-receiving (Sect. 3.5) and modulating (Sections 2.10, 2.13, 3.21, 4.10, 6.18) interferences the material will not be supplemented.

A. Active masking interferences and the principles of protection from them.

§7.2. Natural and mutual masking active jamming and the principles of protection from them.

As already mentioned, to the natural masking active jamming can be attributed the interferences of discrete sources (Sun, the moon, the radio stars, etc.), which create noises together with the distributed in the atmosphere and space radiation sources (see §5.8). Virtually effect on operation of radar stations of SVCh range they can exert the Sun, also, to a lesser degree the moon. The density of the power flux of the Sun (see Fig. 5.32b) at wavelength 10 cm, proves to be order $(10^{-20}-10^{-18})$ W/m$^2$•Hz, where a larger number corresponds to the increased solar activity. This density exceeds the density of blackbody radiation at temperature of 6000°K 10-1000 times. At wavelength 1 m, the density of power flux will be $(10^{-23}-10^{-17})$ W/m$^2$•Hz.

Recently very important role is begun to play interferences. In proportion to a rapid increase in the number of utilized radio-electronic means, sharply grow/rises the danger of their mutual effects. In order to remove these effects, practices the planned distribution of the operating frequencies between different radio-electronic means both on the base of international agreements and on the base of internal regulations within the limits of each country, each branch of national economy and military science.

Page 423.

Nevertheless, in the absence of proper protective measures from interferences is observed the mutual effect of radio-electronic means even with different operating frequencies. The latter occurs when the extraband and spurious radiations of radio-electronic means are present,.

Extraband are called emission/radiations in the vicinity of the nominal operating frequency, which emerge beyond the limits of the diverted frequency band. Secondary include the emission/radiations at harmonics, subharmonics, and also combination frequencies (in the case of using the driver with frequency conversion). Together with extraband and spurious radiations the reason for interferences are the supplementary channels of reception/procedure in superheterodyne receiving equipment/devices. It is known that under the influence on the mixer of the incoming variations of frequency f and of the fluctuations of the heterodyne of frequency $f_г$ at the output of mixer are formed the fluctuations of a series of combination frequencies $|nf \pm mf_г|$. If any of these frequencies coincides with the intermediate, to which are inclined the subsequent cascade/stages of receiver, it is amplified and is formed the supplementary channel of

reception/procedure. Under the actual conditions when $f_r \gg f_{пр}$ the supplementary channels of reception/procedure are formed at frequencies of input oscillations $f_{mn} = \frac{1}{n}(mf_r \pm f_{пр})$. Directional characteristic of the receiving and transmitting antennas for extraband emission/radiations, spurious radiations and the channels of reception/procedure usually differ from directional characteristic for the fundamental channels of emission/radiation and reception/procedure, in the first place, in terms of considerably high side-lobe level.

In many instances can be created fairly complicated situation. It is real/actual, in one and the same area, the transmitters of radio-electronic means create fundamental, extraband and spurious radiations, and the receptors of these means together with fundamental have the supplementary channels of reception/procedure. If the fundamental or supplementary channel of reception/procedure randomly coincides with the fundamental or supplementary channel of emission/radiation and the intensity of the emitted oscillation is sufficiently great, can occur interference, which in particular masks.

Thus, for instance, frequency modulated and amplitude-modulated continuous fluctuations of the communication lines can create the masking interference with pulse radar receivers. To narrow-band

Doppler receivers the masking interference they can create not only line of communication, but even radio aids, the radiating momentum/impulse/pulses, since the latter are dilate/extended in narrow-band duct/contours.

Page 424.

The aggregate of the measures, directed toward the exception/elimination of interferences, provides electromagnetic compatibility. Together with by correct allocation of frequencies and by other organizational actions electromagnetic compatibility is reached because of the filtration of spurious radiations in transmitters, heterodyne vibrations in receiving circuits, because of the correct use of conditions of propagation, special feature/peculiarities of locality, selection of the modes of operation of radio-electronic means.

The aforesaid here relative to the mutual masking interferences in many respects is related also to the mutual by those imitating interferences which are examined further in §7.19-7.21.

§7.3. Artificial masking active jamming, the special feature/~~peculiarities~~ of their effect and methods of designing.

As the artificial masking active jamming can be used the emission/radiation of noise oscillation/vibrations. Noise oscillation/vibrations can be created intentionally both by the separately excited generators and self-excited oscillators, which is more economical, for example by the special magnetrons, working in the noisy conditions/mode.

With the sufficiently large dynamic range of the receiver, noise oscillation/vibrations create the effect, analogous to a sharp increase in the internally-produced noise, which impedes detection and a change in the parameters of radar signal at large target ranges. Very powerful artificial active jamming, as mutual, can act in principle and along the secondary channels of reception/procedure.

If the dynamic range of receiver is insufficient and occurs amplitude limitation (especially in the last intermediate-frequency amplifier stages, after the contraction of passband), relation of signal-interference after limiter even more deteriorates. This is explained in Fig. 7.1, is shown the passage through the limiter of the unmodulated harmonic interference together with the signal pulse.

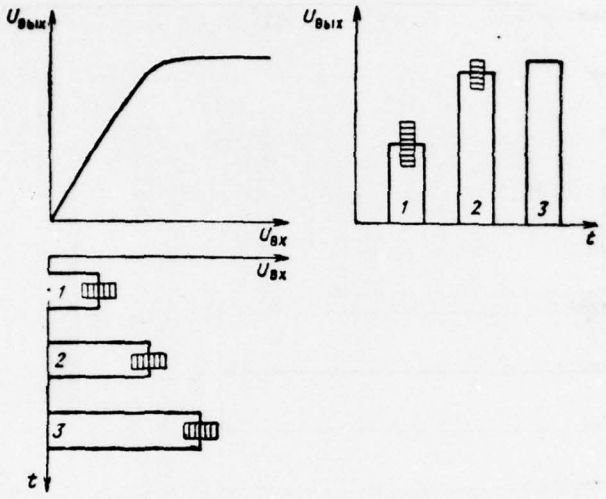


Fig. 7.1. Effect of weak (1) and powerful (2, 3) interference on the passage of signal.

Page 425.

It is evident that with an increase in the jamming intensity can occur the complete suppression of signal. Analogous effect occurs also in the case of the effect of noise interference with the insufficient dynamic range of receiver. Therefore the effect of the masking interference with the low dynamic range of receiver is especially dangerous. But even with the very large dynamic range of receiver the effect of interference, equivalent to an increase in the internally-produced noise, can considerably impair or completely tear

away radar detection or tracking.

For simplification of the equipment for the creation of interferences together with the generation of noise, is utilized the generation of the oscillation/vibrations, modulated by noise in amplitude or frequency. Thus, for instance, frequency-modulated oscillation

$$u(t) = U\cos\left[\omega_0 t + \int_0^t \Delta\omega(t)\,dt\right], \qquad (1)$$

where $\Delta\omega(t)$ – random modulating function, will be the frequency modulated by noise interference, if a change in the frequency $\Delta\omega(t)$ occurs in accordance with certain noise oscillation.

To a number of the electronic devices, which make it possible comparatively it is simple to carry out frequency modulation, are related carcinotrons. Supplying to carcinotron through the video amplifier noise oscillation from noise generator (for example, on thyratron in magnetic field), it is possible to obtain the frequency modulated oscillation of form (1). Contemporary carcinotrons allow/assume frequency deviation, beginning from unity to hundred megahertz, that makes it possible to create the interferences in a comparatively wide and narrow frequency spectrum, called respectively barrage and aiming.

From the fundamental pcint, the modulated by noise interference is not completely equivalent tc internally-prcdtced noise of receiver, especially, if it is generated in brcadband of frequencies. For nqise with the unifcrm spectrum, are nct virtually correlated the instantaneous values of voltage through the interval of order 1/Δf, where Δf - frequency band. Meanwhile for the modulated by noise interference not correlated will be the values, divided by interval $1/\Delta F_{\text{мод}}$, where $\Delta F_{\text{мод}}$ - width of the spectrum of the modulating oscillations. Nevertheless, under the influence on receiver with a band less $\Delta E_{\text{мод}}$ and tc the deviatien cf frequency, the interference, frequency-modulated by ncise, creates virtually the same effect as noise interference. In this case for transit time in narrow-band receiver, is superimposed a series cf the independent effects, which correspond to the incidence/impingement of instantaneous frequency into the passband cf receiver.

Page 426.

The statistics of the sum of the superimposed instantaneous values at each moment of time approaches in this case Gaussian, the law of amplitude distribution becomes Rayleigh, correlations proved to be the same as for the noise, passed through the narrow-band oscillatory system.

Both noise and modulated by ncise jamming transmitters they can additionally be retuned (to slip in frequency). The obtained with this interference is called sliding.

The sliding interference is clearly transient random process. However, even nonslipping interference in real conditions of effect also incompletely is reduced to staticnary process. Thus, for instance, directional characteristic of survey radar modulates not only signal, but also interference.

However, in a series of cases, the transiency of interference is not decisive. Specifically, for such cases will be given below the analysis of detection conditions against the background of the active masking interferences.

§ 7.4. Equation of radar, the range and visibility range RLS under the influence of the masking staticnary active jamming.

With sufficient dynamic range of receiver, the condition of target detection in the masking stationary active jamming of the type of white noise takes the form

$$\mathcal{E}_{пр} \geqslant \nu (N_0 + N_{пом}), \qquad (1)$$

where $\mathcal{E}_{пр}$ - energy of received signal at the input of receiver of RLS; $\nu$ - coefficient of discernability of preset parameters of detection or measurement; $N_0 = kT\text{Ш}$ - spectral density of internally-produced noise of receiver; $N_{пом}$ - the spectral density of the masking interference at the input of receiver.

If the input of receiver affect oscillations from several producers of the active jamming (i=1, 2, 3, ..., m), then

$$N_{пом} = \sum_{i=1}^{m} \frac{1}{4\pi} \frac{P_{пi} G_{пi} A_i'}{r_{пi}^2 \Delta f_{пi}} \gamma_i \alpha_i. \qquad (2)$$

Here: $P_{пi}$, $\Delta f_{пi}$ - power of noise and the width of its energy spectrum; $G_{пi}$ - value of the antenna gain in direction on RLS for the i jammer; $A_i'$ - effective area of receiving antenna in direction to i producer of interferences; $r_{пi}$ - distance from RLS to the i producer; $\gamma_i$ — coefficient, which considers a difference in the polarization of the interference, which comes in from the i jammer, and the polarization, optimum for the receiving antenna (are taken values from 1 to 0); $\alpha_i$ — coefficient, which considers possible deterioration in the

quality of interference from the i producer because of the use of modulation by noise (for noise interference $\alpha=1$). The entering expression (1) value $\vartheta_{пр}$ is determined from [(3), §5.4].

Page 427.

If the maximum radar range in interferences, as earlier, to designate $r_{макс}$, that, by replacing inequality (1) by equality, we pass to the equation of radar in the presence of the interferences

$$\frac{\vartheta G \sigma A}{(4\pi r_{макс}^2)^2} = v\left(N_0 + \sum_{i=1}^{m} \frac{1}{4\pi} \frac{P_{пi} G_{пi} A_i'}{r_{пi}^2 \Delta f_{пi}} \gamma_i \alpha_i\right). \qquad (3)$$

Sometimes this equation calls equation radar countermeasures.

Utilizing an equation radar countermeasures, distinguish the following conditions/modes of the cover of signal from target/purpose by interference; self-covering, external and collective cover.

Self-covering it is possible to call/name the case when target/purpose is covered by jamming transmitter, placed on its edge. With external covering it is possible to call/name the case when the quiet target/purpose is covered by jammers, collective - when interferences are placed from the edge of target/purpose from other producers.

Noting that in the case of self-covering n=1, $r_{n1} = r_{макс}$, $A_1 = A$, and designating relation to the maximum range in the presence and absence of interferences $\frac{r_{макс}}{r_{0макс}} = y$, expression (3) we bring to the biquadratic equation

$$y^4 + y^2/a^2 = 1. \qquad (4)$$

Here a is relation to the range in interferences $r'_{макс}$ to range without interferences when the range in interferences is determined disregarding by internally-produced noise of receiver. For this last/latter case from equation (3) we obtain:

$$r'_{макс} = \sqrt{\frac{\Im G \sigma \Delta f_п}{4\pi P_п G_п \nu\gamma\alpha}}. \qquad (5)$$

Solution of biquadratic equation (4) is given by the expression

$$y = \sqrt{\frac{1}{2}\left[\sqrt{1/a^4 + 4} - 1/a^2\right]}$$

and by the curve/graph of Fig. 7.2, which makes it possible to find correction to solution (5), obtained disregarding by internally-produced noise. However, in the majority of the cases,

correction is not caused by need, since $a \ll 1$, $y = a$ and $r_{макс} = r'_{макс}$.

Page 428.

For the conditions/mode of external cover, is characteristic the difference for values $A_i'(\beta, \varepsilon)$ from value A. This is most noticeable when antenna is turned away from producer of interferences and interference operates on the minor lobes of radiation pattern. If antenna completes survey/coverage, for example, along azimuth, then $A(\beta,\varepsilon)=A_{макс}F^2(\beta-\beta_0, \varepsilon)$, where $\beta_0$ - direction of the axis of radiation pattern. Let the target/purpose be located on azimuth $\beta_0$, and the source of interference on azimuth $\beta_i$, then the corresponding values of effective antenna area will be $A = A_{макс}F^2(0, \varepsilon)$ and $A_i' = A_{макс}F^2(\beta_i-\beta_0, \varepsilon)$. Substituting these expressions in (3) for each azimuth, it is possible to determine the range, and also, therefore, to establish/install visibility range for this angle $\varepsilon$.

The exemplary/approximate form of visibility range in the case of two producers of interferences is shown on Fig. 7.3. Is observed a reduction in the range in comparison with the case of the absence of interferences, even when interference operates on lateral lobes of radiation pattern. A great reduction in the range occurs in direction on jammer. In the vicinities of direction on jammer can be created the sectors of effective suppression. The degree of the

decrease of range in each case as, as the width of the sector of suppression, depends on the parameters of radar.

If we analogously investigate the dependence of range on $\varepsilon$ then it is possible to ascertain that only does not decrease the range, but also descends the ceiling of detection and rises the lower edge of visibility range.

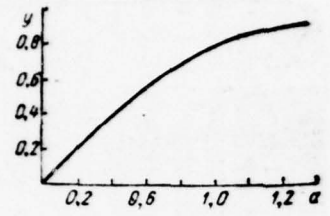


Fig. 7.2. On the calculation of the range during self-covering on a precise formula.

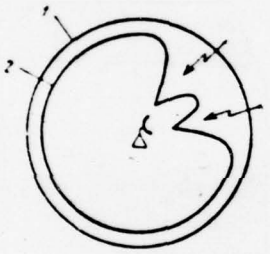


Fig. 7.3. Visibility ranges of RLS in the absence (1) and under influence of interferences from two directions (2).

Fig. 7.4. Form of PPI scope under influence of interferences from two directions.

Page 429.

The given examination concerned RLS with the sufficiently large dynamic range of receiving circuit, for example with automatic gain control on the level of interference. If this is not observed, then together with the loss of the possibility to spot a target at long range will be lost the possibility of target detection and at short distances, since the interference level can exceed the level of limitation in the circuit of receiver. For the case, depicted in Fig. 7.3, in the absence of automatic gain control and the insufficient dynamic range of receiver on indicator will be observed the picture, shown on Fig. 7.4.

§7.5. Possible principles of protection from the masking active jamming.

Protective measures from the masking active jamming can be sufficiently effective only in such a case, when does not occur the suppressions of signal because of the insufficient dynamic range of receiver. In this case, can be accepted the number of the measures, connected, for example, with the use of the frequency, three-dimensional/space, polarization selection, etc.

As can be seen from expressions (1) and (3), to an increase in the range in interferences will contribute all measures, increasing the left and decreasing the right side of these expressions. Thus, for instance, increase in the energy of the sounding signal makes it possible to increase the range in interferences proportionally $\sqrt[4]{\ }$ in the mode of external cover and $\sqrt{\ }$ — in the conditions/mode of self-covering. An increase of the factor of amplification of the transmitting antenna in direction in target/purpose makes it possible to increase the range in interferences also proportionally $\sqrt[4]{G}$ in the conditions/mode of external cover and $\sqrt{G}$ in the conditions/mode of self-covering.

The decrease of polarizational coefficient $\gamma$ sometimes can lower the effect of interference in comparison with the effect of signal. The decrease of the coefficient of discernability $\nu$ also contributes to the solution of this problem. As a whole, the range of action in the conditions/mode of self-covering is proved to be inversely proportional $\sqrt{\gamma}$ and $\sqrt{\nu}$. Finally, the decrease of the relative level of lateral lobes of radiation pattern A'/A (or even the formation/education of failures in major lobe in direction in the sources of interferences) makes it possible to increase the range in the conditions/mode of external cover proportionally $\sqrt[4]{A'/A}$.

Page 430.

Let us turn to somewhat more detailed examination of the enumerated above possibilities. An increase in the energy of the scunding signal can be realized via the increase of power and increase in the duration of signal. Energy of the sounding signal will be rationally utilized for reception/procedure only in the case of approaching treatment/working the adopted oscillations to the optimum (otherwise grow/rises value $v$ in the right side of equality).

An increase of the antenna gain in direction in target/purpose, creating the concentration of useful energy, can b the same time retard survey/coverage of space, if this concentration will be in equal measure provided for all directions. As has already been indicated in §5.5, are developed at present the methods of controlled survey/coverage with the sequential analysis when the time during which the antenna is directed toward target/purpose, depends t of detection conditions and, in particular, on interference situation. Especially great possibilities for using programmed automatically controlled survey/coverage are open/disclosed during the application/use of the transmitting antennas with electronic beam

control in the form of the phased gratings. In §5.5 were given published in the literature the data of the simulations, according to which the gain during the use of a sequential analysis in the case of the different effect of interferences from different directions is especially great (5-22 dB).

It is known that the receiving antenna is usually inclined to some specific polarization of the received signal: linear, circular, or in the general case elliptical. Are possible antennas with the adjustable polarization. If antenna polarization is establish/installed the corresponding polarization of interference, the effect of the action of interference will be greatest. Thus, for instance, for the vertical polarization of interference effect will be greatest, if reception/procedure is conducted to vertical vibrator; for circular polarization with the rotation of the vector of field clockwise the effect of action will be greatest, if antenna is designed to this same the form of polarization. Knowing this fact, antenna it is possible by the fact or in another manner to change for orthogonal polarization, i.e., for the given examples - to horizontal, or for circular polarization, but with rotation counterclockwise. For elliptically polarized wave orthogonal is also elliptically polarized oscillation, but with the shifted on 90° position of the ellipse of polarization. In all cases indicated it is possible to attain the essential weakening of interference. Will be

or will not occur in this case respectively the weakening of useful signal, it depends on the polarization of the oscillations of signal. If the polarization of the oscillations of useful signal coincides precisely with the polarization of the oscillations of interference, simultaneously with interference and in the same measure will be attenuate/weakened signal. Since (even during the fixed for emission/radiation polarization) the polarization of the signals, reflected from actual targets, is random, in the general case not coinciding with polarization of interference, there are possibilities in principle to attenuate/weaken interference greater than signal.

Page 431.

For the increase of interference shielding, it is expedient to decrease the coefficient of discrimination $\nu$ in [(1), §7.4]. The decrease of coefficient $\nu$ is achieved because of the approach/approximation of reception/procedure to optimum. If interference is stationary noise interference of the type of white noise, then decrease $\nu$ is achieved by the already examined optimization of reception/procedure for such interferences. With filter reception/procedure this, in particular, indicates the use of an optimum frequency characteristic, i.e., optimum frequency selection. Frequency selection is more effective, the wider the interference spectrum in comparison with the spectrum of signal,

i.e., if interference is barrage ir frequency. In this case the spectral jamming density at the assigned power of jamming transmitter descends inversely proportional to the noise band. Spot jammings (with the smaller frequency band), as a rule, are more effective, but to with more difficulty realize them. The creation of spot jammings in the greatest measure hinders in the case of the rapid retuning of the frequency of radar, with the multifrequency or broadband sounding case, etc. If the noise band is considerable already of the width of the spectrum of received signal, then the resulting noise it is not possible to consider white. In this case of optimum, is frequency characteristic with suppression in the noise band or, in other words, expediently the use of various kinds of the tuned band rejection filters for the oscillations of interference, which leads to the essential decrease of the coefficient of discernability $\nu$ (see §7.8).

A decrease in the side-lobe level of radiation pattern can noticeably attenuate/weaken interference effect and is the independent problem, especially important in the case of external cover. From the theory of antennas, it is known that a decrease in the level of lateral lobes can be reached because of an increase of the size/dimensions of antenna, rational field distribution into aperture, the increase of the precision of manufacturing, decrease in the effect of re-reflection from the adjacent objects. The increase

of the selectivity of antenna can be attributed to the category of an improvement in the three-dimensional/space selection of received oscillations.

For an improvement in the three-dimensional/space selection of signal against the background of the interferences, which come in from separate directions, can be also in principle used the described in the literature methods of the incoherent and coherent compensation interference oscillations. For this, together with fundamental can be begun to operate supplementary antennas (in antenna of the type the phased grating - separate cell/elements of this grating). The possibilities of the compensation interferences were formulated by Soviet scholar N. D. Papaleksi still several decades ago [9].

Page 432.

If signal, received by supplementary antenna, compensates for the signal, taken on lateral lobes of fundamental antenna, after detector, one should speak about incoherent compensation. If this compensation is conducted at high (intermediate) frequency, it is possible to call it coherent.

Figures 7.5 schematically shows the system, which includes the main and two supplementary antennas. To each antenna corresponds its

channel of reception/procedure. The oscillations, passed through the corresponding channels of reception/procedure, are supplied to summator. In this case, at least in two supplementary channels in amplitude and phase are regulated composite transmission factors $K_1$ and $K_2$. If composite directional characteristic of channels take form $F_0(\theta)$, $F_1(\theta)$, $F_2(\theta)$, then total composite directional characteristic can be presented in the form

$$F_\Sigma(\theta) = F_0(\theta) + K_1 F_1(\theta) + K_2 F_2(\theta). \qquad (1)$$

Then for the angular coordinates of the sources of interferences $\theta_1$ and $\theta_2$ it is possible to attain the formation/education of failures in resulting directional characteristic for these directions. Those necessary for this value $K_1$ and $K_2$ are determined from system of equations

$$\begin{aligned} F_0(\theta_1) + K_1 F_1(\theta_1) + K_2 F_2(\theta_1) &= 0, \\ F_0(\theta_2) + K_1 F_1(\theta_2) + K_2 F_2(\theta_2) &= 0. \end{aligned} \qquad (2)$$

Failures in directional characteristic, formed because of the coherent compensation interferences, create the supplementary reserve of the three-dimensional/space selection of the interferences, which

affect both of the main thirg and cf lateral lctes of directional characteristic. Especially wide scope fcr applying the compensation methods is open/disclosed during the use of receiving antennas in the form of the phased gratings.

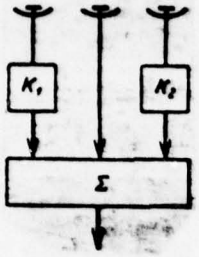


Fig. 7.5. System with two supplementary receiving channels for forming failures in the resulting radiation pattern.

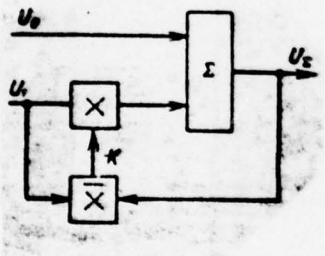


Fig. 7.6. Diagram with correlation feedback.

Page 433.

The selection of coefficients in multichannel diagrams, similar to diagram in Fig. 7.5, it is possible to accomplish, by utilizing principle of correlation feedback.

Figure 7.6 shows diagram with two inputs which enter the

voltages one and the same of frequency with composite amplitudes of $U_0(t)$ and $U_1(t)$ (for example, from fundamental and supplementary antennas). On summator is formed the voltage

$$U_\Sigma(t) = U_0(t) - K U_1(t). \qquad (3)$$

There is a feedback loop with the output of summator to controlled member - multiplier in the circuit of the supply of the first voltage. In this circuit is included the equipment/device of the computation of the estimate/evaluation of covariance $\overline{U_\Sigma U_1^*}$. The latter with an accuracy to constant $\chi$ is utilized as the governing factor K, supplied to controllable cell/element. From two equations: $K = \chi \overline{U_\Sigma U_1^*}$ and (3), it is possible to find

$$K = \frac{\chi \overline{U_0 U_1^*}}{1 + \chi |\overline{U_1}|^2}, \qquad (4)$$

$$U_\Sigma = U_0 - \frac{\chi \overline{U_0 U_1^*}}{1 + \chi |\overline{U_1}|^2} U_1. \qquad (5)$$

It is easy to see that during $\chi \to \infty$ and the sufficient correlation $U_0$ and $U_1$ (for example, when $U_1 = CU_0$, where C=const) occurs the complete compensation, i.e., $U_\Sigma$ it is turned into zero. The multiplication of complex amplitudes, as is known, can be

realized, for example, via conversion of frequency, averaging - because of integration in narrow-band filter (§3.16). The same process/operations can be produced by analog quadrature perfecting (§3.8) or of transition to digital computer technology.

The compensation effect interference is provided, if correlation feedback enveloped each of the inputs of diagram. So that the voltage $U_0$ would enter in this case to the output of summator in the absence of the correlated interference when control voltage - $K_0$ is turned into zero, to it leans weight voltage $\alpha$.

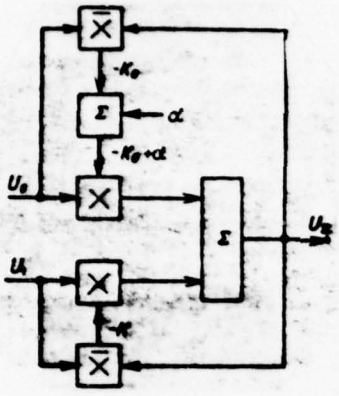

Fig. 7.7. Diagram of compensation with correlation feedback at both inputs.

Page 634.

Initial equations then take the form:

$$U_\Sigma = (-K_0 + \alpha) U_0 - K U_1, \tag{6}$$

$$K_0 = \chi \overline{U_\Sigma U_0^*}, \tag{7}$$

$$K = \chi \overline{U_\Sigma U_1^*}. \tag{8}$$

Substituting (6) in (7) and (8), it is easy to obtain system of equations:

$$K_0(1+\chi\overline{|U_0|^2})+K\chi\overline{U_1U_0^*}=\alpha\chi\overline{|U_0|^2},$$
$$K_0\chi\overline{U_0U_1^*}+K(1+\chi\overline{|U_1|^2})=\alpha\chi\overline{|U_1|^2}. \quad (9)$$

During $\chi\to\infty$, $\alpha=\alpha_0=\text{const}\neq 0$ and the total correlation of voltages $U_0$ and $U_1$, when $U_1=CU_0$, from (6) and (9) we will obtain that $U_\Sigma\to 0$, i.e. this diagram, as preceding/previous, can realize the compensation interferences.

Together with the compensation interference, both of diagrams can realize the compensation signal, if the duration of the latter is sufficient for the retuning of diagram. In the case of very short signal the first, and second diagrams will be inclined only for the compensation interference. It is easy to see that in the absence of interference both of diagrams give the values of the governing factors K and $K_0$, equal to zero. The output voltage of the second diagram in this case $U_\Sigma=\alpha U_0$, i.e. in the absence of interference each of the diagrams passes the oscillation, which comes in along fundamental channel. With $\alpha=1$ both of diagrams, are identical. It is easy to understand that if in diagram (Fig. 7.7) $\alpha=\alpha_0$, and in its lower part to the voltage of correlation feedback - K will be added the weight $\alpha_1$, then output effect in the absence of interferences will be

$$U_\Sigma=\alpha_0U_0+\alpha_1U_1.$$

On the basis of that presented, without giving more detailed lining/calculations, it is possible to understand one of the possible schematics of the construction of self-tuning of an antenna of the type the phased grating (Fig. 7.8) [152]. In each of the cell/elements of the phased grating, is utilized correlation feedback. In the diagram the correlation feedback is shown only for extreme (left and right) cell/elements. Terms $\alpha_1, \alpha_2, \ldots, \alpha_m$ provide the best effect of the reception of signal in the absence of interferences (they analogous of component $\alpha$ in diagram in Fig. 7.7). In the presence of the interferences, arriving not more than from m directions, is possible the formation/education of failures in directional characteristic, in these directions. As is shown detailed analysis for the discrete case (similar given in Appendix 9 with continuous antenna), forming directional characteristic is optimized taking into account interferences, providing the most advantageous three-dimensional/space selection.

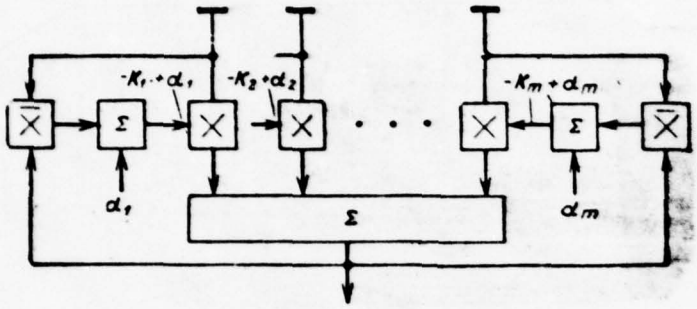


Fig. 7.8. Multichannel schematic of the compensation interferences with the use of correlation feedback.

Page 435.

B. Passive masking jamming and the principles of protection from them.

§ 7.6. Passive masking jamming and methods of its creation.

As has already been indicated above, the natural passive interferences include the radio interferences, created by natural reflectors (ground features, water surface, hydrometeors, the aurora borealis, etc.). These interferences can substantially upset the operation of the airport radars, which ensure landing, and radars of military designation/purpose, utilized for target detection, especially at low altitudes.

Widest use from the artificial masking passive interferences received the interferences, created by dipole confusion reflektors. As noted in § 2.5, they are the passive half-wave vibrators, prepared from chaff, foil or the metallized glass and kapron filament. The

length of narrow-band electrodynamic shakers is selected approximately an equal to half wavelength of suppressed RLS. The width of belts depending on their length can be within limits from several millimeters to several centimeters, and the diameter of filament - from ten to hundred microns with the thickness of the metallic coating of the order of ones of microns.

Usually dipole reflectors are collect/built into packets in this quantity that each packet according to its reflecting properties would imitate actual target $(\bar{\sigma}_n = \bar{\sigma}_u)$. The number of reflectors in packet n depends on the wave band in which works suppressed RLS, and can be determined in accordance with [(5). and (6), § 2.5]:

$$n = \bar{\sigma}_u / 0{,}17\lambda^2.$$

Page 436.

Main disadvantage in such packets - narrow range of overlapped frequencies (5-10o/o) from resonance). The frequency band can be expanded, if packets are completed from the vibrators of different length or are increased length and the transverse size/dimensions of dipoles. Packets can be placed between the special belts which are coiled around the drums, arrange/located in cassettes. With them can equip itself antiradar receptacles. Recently appeared the report/communications against developments abroad of equipment for

the creation of passive jamming with the cutting of the dipole reflectors on board aircraft in dependence on that reconnoitred the frequency band of suppressed RLS.

For the masking of aerial targets, the dipole reflectors are dumped in the surrounding space on the aid of automatic machines and bombs (into rear hemisphere) or are detonated with the aid of guns and rockets (into front/leading and rear hemispheres). In this case, they can be created both continuous bands (cloud) of passive reflectors and the breaking.

The cloud of reflectors is characterized by its density. The density of passive reflectors, determined by a quantity of packets per unit of path, with flight on or from RLS is located through the formula

$$m_1 = \frac{z}{v_u t_{cop}}, \qquad (1)$$

where z - a number of automatic machines of the dropping of reflectors; $v_u$ - speed of producer of interferences; $t_{cop}$ - time between the jettisoning of the packets of dipoles.

Knowing the density of dipoles, it is easy to calculate a quantity of packets in one pulse space

$$m_{\Delta r} = m_1 \Delta r,$$

where $\Delta r$ - range resolution of suppressed RLS.

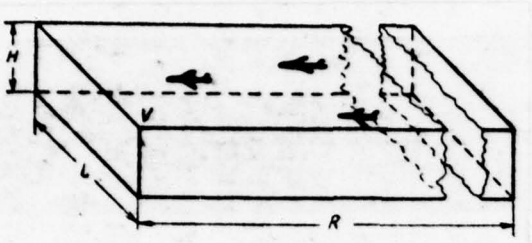


Fig. 7.9. Explanation to the calculation of a quantity of packets in space V.

Page 437.

If with passive jamming is masked volume V of space, in which the system of of those spread on azimuth and angle of elevation of aircraft passes distances of R (Fig. 7.9), then a quantity of packets, jettisoned into this space, is determined by the expression

$$m_{R,L,H} = m_{\Delta r} \frac{R}{\Delta r} \frac{L}{r\Delta\beta} \frac{H}{r\Delta\varepsilon}, \qquad (2)$$

where R, L, H - size/dimensions of the disguisable space V; $\Delta r$, $r\Delta\beta$, $r\Delta\varepsilon$ - size/dimensions of pulse space of RLS at a distance of r from station.

For the masking of target/purposes, it is necessary that the

average/mean effective surface of the dipoles, which occupy pulse space of RLS, would exceed the average/mean effective surface of target/purposes, which were being found in this space. Disregarding the mutual screening of the dipole reflectors, and also by their strain and destruction with dropping, it is possible to determine the average/mean effective surface of the cloud of the dipoles, which occupy pulse ones space, by the formula

$$\overline{\sigma_{пп}} \approx 0{,}17\lambda^2 nm_{\Delta r} = \overline{\sigma_п} m_{\Delta r}.$$

The condition of suppression of RLS, by that not shielded from passive jamming, it is possible to record in the form

$$\overline{\sigma_{пп}} > \overline{\sigma_п}/\nu, \qquad (3)$$

and for shielded RLS

$$\overline{\sigma_{пп}} > \overline{\sigma_п} K_{пп}/\nu, \qquad (4)$$

where $K_{пп}$ - a coefficient of the subclutter visibility of protection equipment (§ 7.18), and $\nu$ - a coefficient of discernability.

§ 7.7. Fundamental differences for the signals of target/purposes and masking passive interferences.

The echo from target/purposes signals and the masking passive interferences have the specific differences, connected with the differences of target/purposes and reflectors, which create passive

jamming. To a number of these differences, can be attributed:

1. Distributed character of the mixing reflectors and close to that concentrated - the bright cell/elements of target/purpose. Therefore, by raising resolution on coordinates and by reducing in this case the size/dimensions of the solved space (in any case, to the size/dimensions, which exceed the size/dimensions of aircraft), it is possible to attain an improvement in the observability of signal against the background of passive jamming.

2. Differences in polarization of echo signals are observed, if passive jamming is created, for example, by hydrometeors (rain, cloud), which consist of small drops, which have form of sphere. If hydrometeors are irradiated by oscillations with circular polarization, then they reflect oscillations also with circular polarization, but with the reverse (if is looked in the direction of propagation of wave) rotation of the plane of polarization.

Page 438.

If receiving antenna does not receive oscillation with this polarization, it nevertheless can accept oscillations from the target/purposes, which possess the asymmetry of structure (§ 2.15).

3. Differences in rate of displacement/movement of interfering reflectors and target/purpose. The rate of the displacement/movement of the ground-based mixing reflectors of relatively ground radar is equal to zero, while the being of practical interest target/purposes they are moved with sufficiently high rate.

If passive jamming is created by the confusion reflektors, then these reflectors, being are discarded from aircraft, rapidly lose initial rate, acquiring the rate, close to wind velocity. Since wind velocity is not constant on height/altitude, in accordance with a high-altitude jump/drop (gradient) in this velocity, occurs the velocity spread of the confusion reflektors.

Nevertheless, differences in the radial velocity of target/purposes and reflectors are and can be used for a selection on velocity. Selection on velocity (otherwise on the effect of the motion of target/purpose) calls the selection of the driving/moving target/purposes (SDTs).

At base of SDTs lie/rests the phenomenon of the strain of the structure of signal with reflection from the driving/moving target/purpose (see § 2.9). This phenomenon is illustrated in Fig. 2.16 for the simplest single radio pulse and in Fig. 7.10 for the sequence of short radio pulses. Figures 2.16, for example, shows the

curve/graph of the motion of target/purpose and the curve/graphs of the propagation of beginning and end/lead of the momentum/impulse/pulse. It is possible to ascertain that during the motion of target/purpose from radar proceeds an increase in the duration of entire pulse and period of high-frequency oscillations $\frac{c+v_r}{c-v_r} \approx (1+\frac{2v_r}{c})$ once (see § 2.9). For a pulse sequence (Fig. 7.10) occurs the extension also of the interval/gap between two adjacent momentum/impulse/pulses into a number once indicated, so that this interval/gap obtains increment $\Delta T = \frac{2v_r}{c}T$. On Fig. 7.11a shown corresponding change in the spectrum for the case of Fig. 2.16, while in Fig. 7.11b - for the case of Fig. 7.10 (on the assumption that all radio pulses of this figure they represent cut of one sinusoid, and the sequence of momentum/impulse/pulses is periodic). In each of the cases indicated to extension along the axis of time $\frac{c+v_r}{c-v_r}$ once corresponds the compression of the axis of frequencies during the motion of target/purpose also $\frac{c+v_r}{c-v_r}$ once. If the width of the spectrum as this is shown on Fig. 7.11a, it is small in comparison with carrier, then the strain of the amplitude-frequency spectrum is reduced to its displacement to certain Doppler frequency $F_д = \frac{2v_r}{\lambda}$. A similar effect is shown on Fig. 7.11b for the comb spectrum of the periodic sequence of radio pulses.

Page 439.

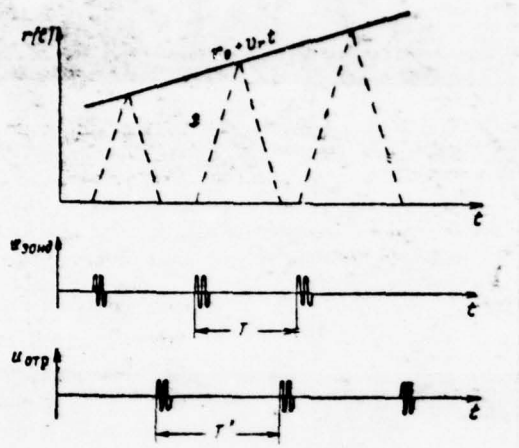


Fig. 7.10. Explanation of transformation of periodic sequence of radio pulses, reflected by driving/moving bright point.

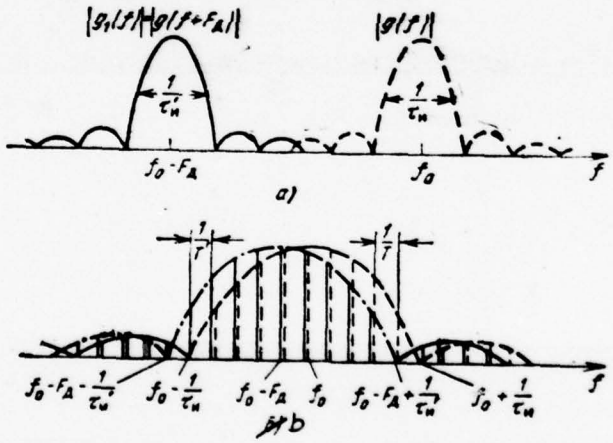


Fig. 7.11. Transformation of spectra of single radio pulse (a) and of periodic sequence of radio pulses (b).

Page 440.

Numerically change in pulse separation because of the high-speed/velocity strain of signal is small. For example, for $\tau=10^{-3}$ s, v=150 m/s and $c=3\cdot10^{8}$ m/s it is $10^{-9}$ s, i.e., the value of the same order as the period of high-frequency oscillations. This means that the strain of signal can be noted only with respect to a change in the phase of high-frequency oscillations. In order to utilize this possibility, are presented sufficiently stringent requirements for the phase structure of high-frequency oscillations, otherwise - to their coherence.

They distinguish several forms of the provision for coherence of oscillations.

1. True internal coherence is reached by fact that oscillations are created by stable master oscillator, after which will cost power amplifier with stable phase response.

2. Equivalent internal coherence is reached by fact that

self-excited oscillator develops sequence of momentum/impulse/pulses of constant carrier frequency with random initial phases. The initial phase of each sounding pulse is memorized during the period of the reception of the echo signals to following sounding. By the corresponding perfecting of the adopted oscillation this phase is eliminated and the adopted oscillations are proved to be by virtually the same, as in the case of true coherence.

3. External coherence is reached by fact that information about random initial phase of sounding pulse is extracted from incoming from passive reflectors oscillations.

The principles of the technical realization of equivalent internal and external coherence are in greater detail developed further. Thus far this will not be stipulated especially, let us propose subsequently that occurs the true internal coherence.

If the secondary emitters, which have different velocities, are permitted on range and angular coordinates, then independent of the form of coherence, the problem of selection in velocity consists of the development/detection of time/temporary (phase) or spectral differences for different sections of space. For example, for the signal of Fig. 7.10 one should determine, there is or there is no displacement of the spectrum for the Doppler frequency, which

corresponds to the radial velocity of target/purpose $F_{au}$.

Considerably more complex is the problem of the selection of the driving/moving target/purposes when target/purpose and the mixing reflectors are located in one elementary solved space. In this case it is necessary to improve the conditions of the detection of signal from target/purpose against the background of passive jamming because of the occurring time/temporary and spectral differences. The latter is reached by the rejection (suppression) of the oscillations of interference and accumulation of signal.

Page 841.

The principle of the rejection of the oscillations of interference lies in the fact that are provided the conditions of its suppression, for example, the spectral components of interferences are cut out (Fig. 7.12). The accumulation of signal lies in the fact that spectral components of signal are processed for purpose of the best isolation/liberation of signal against the background of noises and passive jamming. Since the requirements of rejection and accumulation can prove to be contradictory, for understanding of their optimum relationship/ratio with the selection of the driving/moving target/purposes, can be used the formula of the optimum filtration of signal against the background of nonwhite noise which is set forth in following paragraph.

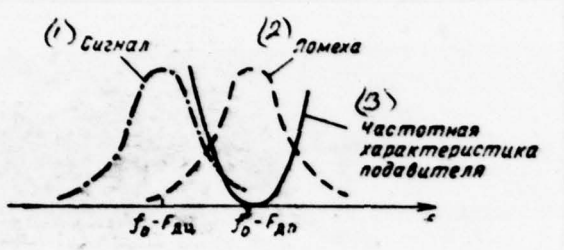


Fig. 7.12. Explanation of the principle of the rejection of interference.

Key: (1). Signal. (2). Interference. (3). Frequency characteristic of suppressor.

§ 7.8. Formula of the optimum filtration of signal against the background of stationary nonwhite noise and its application ~~(appendix.~~

As is known (see § 3.5), stationary random process with uniform spectral density the extra-limited frequency band bears the designation of white noise. If this noise it passes through the linear system from that limited in the frequency band by the amplitude-frequency characteristic, then it can be named nonwhite of noises. Thus, nonwhite noise is characterized by the nonuniform distribution of spectral power density along the axis of frequencies.

The same nonuniform distribution of spectral power density is characteristic also for passive jamming (among other things with the superimposed internally-produced noise). In body itself, if passive jamming in certain pulse space is formed by the reflectors, which have different radial velocity $v_{ri}$ (corresponding to Doppler frequencies $F_{дi}$), then the spectral power density of total interference will be determined by the expression of the form

$$N(f) = \sum_i k_i G(f - F_{дi}) + N_0, \qquad (1)$$

where $k_i$ - the proportionality factor, depending on a number of reflectors in the solved space, which have radial velocity $v_{ri}$; G(f) - the spectral density of interference for motionless reflectors taking into account survey/coverage on angular coordinate; $N_0$ - the spectral density of white noise.

Page 442.

Under specific conditions the maximum of spectral density corresponds to average Doppler frequency $F_{д ср}$. The width of the spectrum depends on the degree of the scatter of velocities and width of the peak of the spectral density of the sounding signal.

Since a number of reflectors and the distribution of velocities can be changed from one solved space to another, in the case of consecutive survey/coverage the range and the azimuth passive jamming

cne shculd consider transient.

Nevertheless, during the study of the possibility of selection within the limits of each solved space transiency is unessential and interference in the first approximation, can be replaced with the stationary nonwhite noise, similar that which is obtained with the passage of white noise through filter [189].

Therefore the which interests us formula will be derived for stationary nonwhite noise. Before approaching toward the derivation of formula let us note that the nonwhite noise unlike white calls the correlated noise. This means that there are such finite time intervals, that the discrete values of voltage, which correspond to the end/leads of these intervals, will be correlated with each other.

Thus, let us derive the formula of the optimum filtration of signal against the background of nonwhite (correlated) steady noise.

Assuming that spectral density N(f) anywhere non-vanishing, let us assume that the noise with a spectral power density of N(f) and signal with a spectral density of stress of g(f) are passed through the filter with the frequency characteristic $K_0(f)$ (Fig. 7.13). The amplitude-frequency characteristic of this preliminary filter let us select so that the spectral jamming density at its output $N(f)|K_0(f)|^2$

would not depend on the frequency

$$N(f)|K_0(f)|^2 = \text{const} = C,$$

or

$$|K_0(f)| = \sqrt{\frac{C}{N(f)}}. \qquad (2)$$

If all values of spectral density N(f) are final, then preliminary filtration will not lead to the loss of any spectral components, i.e., any component of the spectrum can be restore/reduced by the subsequent filtration. Since the noise at the output of preliminary filter became white, optimum detection is realized via the known procedure of filtration against the background of the white noise (see Chapter 3).

Page 443.

Of this filtration must be subjected the useful signal from the output of preliminary filter, which has the composite amplitude-frequency spectrum $g(f)K_0(f)$. Therefore the optimum frequency characteristic of the subsequent filter with an accuracy to constant factor is expressed by the formula

$$K_1(f) = K_{1opt}(f) = [g(f)K_0(f)]^* e^{-j2\pi ft_0}. \qquad (3)$$

Optimum characteristic for the reception of signal against the background of nonwhite noise as a whole will be

$$K_{opt}(f) = K_0(f)K_{1opt}(f) = |K_0(f)|^2 g^*(f) e^{-j2\pi ft_0}$$

or

$$K_{опт}(f) = C\frac{g^*(f)}{N(f)}e^{-i2\pi ft_0}. \qquad (4)$$

The obtained formula of optimum frequency characteristic for the case of nonwhite noise is the generalization of formula for the case of white noise. The latter we obtain from (4), set/assuming $N(f)=N_0=\text{const}$.

Together with the need for the accumulation of the signal, described by the known formula of optimum filtration against the background of white noise, formula (4) considers the need for the rejection when noise is nonwhite. This is illustrated in Fig. by 7.14, where are shown the amplitude-frequency spectrum of signal $|g(f)|$, the spectral power density of the nonwhite noise $N(f)$ and the amplitude-frequency characteristic of optimum filter $|K_{опт}(f)|$. This characteristic testifies to the need for the suppression of the spectral components of noise with the greatest intensity, although in this case simultaneously they are suppressed and the separate spectral components of signal. Resulting amplitude-frequency characteristic $|K_{опт}(f)|$ (Fig. 7.14c) can be presented as product of two amplitude-frequency characteristics of which one $|K_1(f)|=|g(f)\ K_0(f)|$ provides the optimum processing of signal against the background of

white noise, and another $|K_{10}(f)|$ - the rejection (suppression) of the spectral component of adopted oscillations, necessary for the optimization of reception/procedure under conditions of nonwhite noise.

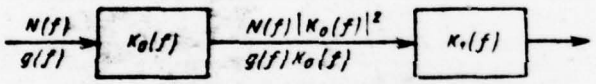


Fig. 7.13. Explanation of the derivation of the formula of the optimum filtration of signal against the background of stationary nonwhite noise.

Page 444.

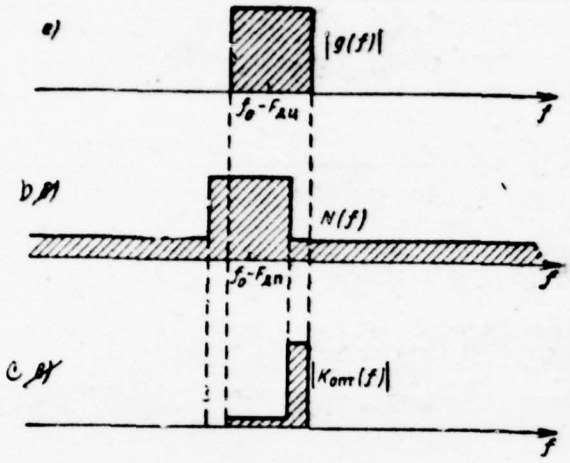


Fig. 7.14. Explanation of formula of optimum filtration: a) amplitude-frequency spectrum of signal; b) spectral jamming density; c) amplitude-frequency characteristic of optimum filter.

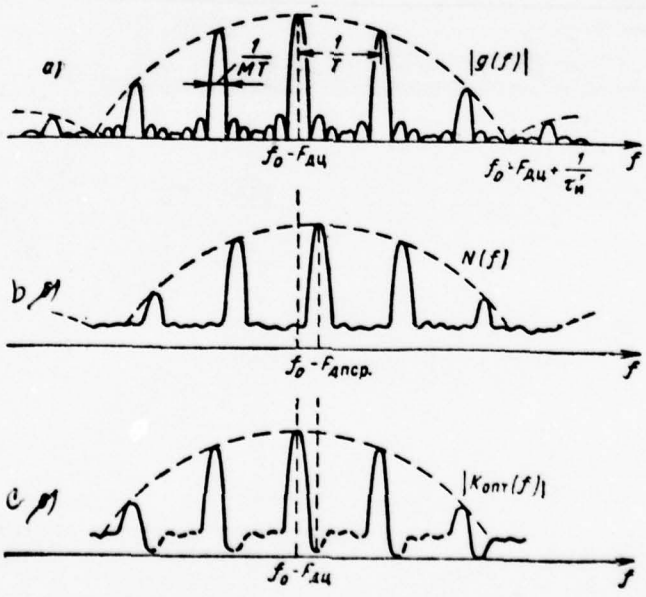


Fig. 7.15. Amplitude-frequency spectrum of packet of radio pulses.

reflected from driving/moving target/purpose (a), spectral jamming density (b), amplitude-frequency characteristic of optimum filter (c).

Page 445.

In Fig. 7.15 is illustrated the application/use of the obtained in this paragraph formulas to the case of the optimum reception of the coherent packet of the periodically following signal pulses in the presence of passive jamming and internally-produced noise. Figure 7.15a depicts the amplitude-frequency spectrum of signal $|g(f)|$, on Fig. 7.15b - spectral density of interference N(f). Presented the curve N(f) is obtained as a result of the shift/shear of the curved spectral density of the sounding signal for the average Doppler jamming frequency $F_{\text{доп ср}}$, of the imposition of components of internally-produced noise $N_0$, and also account of blurring comb interference spectrum because of the velocity spread of reflectors. Figures 7.15c depicts the amplitude-frequency characteristic of optimum filter, which corresponds (4). The conditions of optimum perfecting can be realized, if are consecutively included optimum filter for the single momentum/impulse/pulse of packet, the comb filter of accumulation (for example, in the form of delay line -

recirculator) and finally the comb filter of the suppression of the peaks of interference spectrum (Fig. 7.16). The corresponding frequency characteristics are shown on the same figure.

The first two filters (Fig. 7.16) provide the optimum perfecting of the momentum/impulse/pulses of packet against the background of white noise, the latter - a rejection of interference. In this case, the filter of accumulation is inclined to target speed, and the suppression filter - to the velocity of interference.

The starting process of filters GFP and GFN can be changed, since the product of the amplitude-frequency characteristics in this case is not changed. From the output of filters, the voltage is supplied to detector.

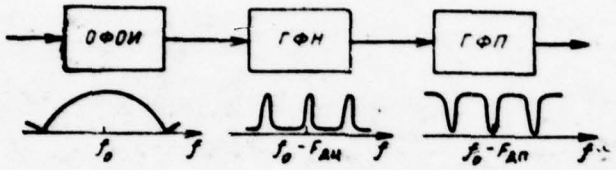


Fig. 7.16. The schematic of the optimum filtration of signal against the background of the nonwhite noise: GFOI - optimum filter of single momentum/impulse/pulse; GFN - comb filter of accumulation; GFP - comb filter of suppression.

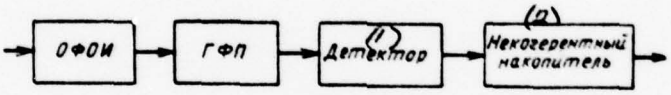


Fig. 7.17. Schematic of optimum processing of signal against the background of nonwhite noise at unknown target speed.

Key: (1). Detector. (2). Incoherent storage/accumulator.

Page 446.

Figures 7.17 shows the modified schematic of the treatment/working in which coherent storage/accumulator is replaced

post-detector (incoherent). During the use of this schematic, is not required the tuning of storage/accumulator to target speed, it suffices to tune the comb filter of suppression by the average speed of interference. The frequency characteristic of pre-detected cascade/stages is determined in this case from the formula

$$K_{опт}(f) \equiv \frac{|g_u(f)|}{N(f)},$$

i.e. it corresponds to the detection of the single radio pulses of incoherent packet against the background of nonwhite noise. Corresponding theories of the comb filters of suppression and accumulation can be comparatively simply realized at intermediate frequency, which shows in following paragraphs. The optimum processing of signal against the background of passive jamming to be carried out and on video frequency, which will be the object/subject of further examination.

§ 7.9. Comb filters of suppression.

If a required number of peaks is great, the realization of filters with the aid of duct/contours produces difficulty. More idle time proves to be the realization of the necessary frequency characteristics with the aid of delay lines.

Figures 7.18a shows the simplest schematic of this filter, which

consists of the line of delay (here at intermediate frequency) and of the generalized summator - schematic of the formation/education of a difference in the undelayed and delayed stresses. This schematic corresponds to the linear process/operations of the processing

$$u_{вых}(t)=u_{вх}(t)-u_{вх}(t-T) \qquad (1)$$

and therefore is linear filter.

The frequency characteristic of this filter can be found from the relationship/ratio

$$K(f)=\frac{u_{вых}(t)}{u_{вх}(t)}\Big|_{u_{вх}(t)=e^{j2\pi ft}}=1-e^{-j2\pi fT}=2je^{-j\pi fT}\sin\pi fT.$$

The amplitude-frequency characteristic

$$|K(f)|=2|\sin\pi fT| \qquad (2)$$

is depicted in Fig. 7.19a. It is turned into zero for frequencies $f_k=\frac{k}{T}$ and it reaches maximum for frequencies $f_k+\frac{1}{2T}$.

The position of zero this characteristics changes during a change in the period of premise/impulse to certain value $\Delta T$.

Page 447.

Since there is the practical interest in the section of comb characteristic within the limits of the band of frequencies of the single radio pulse where value $2\pi f(T+\Delta T)=2\pi fT+\alpha$ can be considered constant, change in position of zeros in the necessary band of

frequencies (dotted line in Fig. 7.19a) can be ensured, by connecting in series with the fixed delay line the adjustable phase inverter.

Let us explain the work of the comb filter of suppression (Fig. 7.18a), assuming that it affect the different sequences of radio pulses (infinite periodic sequence; the packets of periodically following radio pulses, reflected from pinpoint target and from the pulse space of reflectors when velocity spread is present.). Explanation can be given both on the base of the spectral and on the base time/temporary treatment of effect.

The infinite periodic sequence of momentum/impulse/pulses has line spectrum.

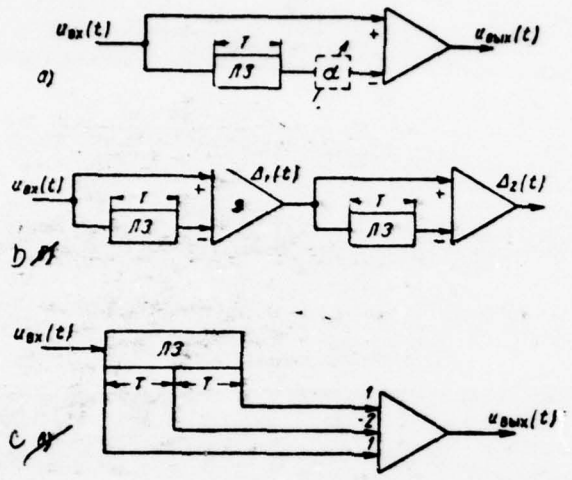


Fig. 7.18. Schematic of single (a) and twofold (b and c) cross-period subtraction - comb filters of suppression.

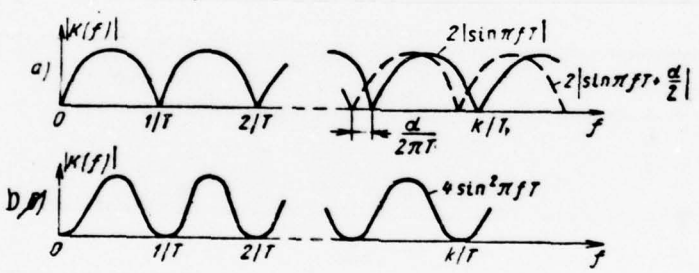


Fig. 7.19. Amplitude-frequency characteristics of schematics of single (a) and twofold (b) cross-period subtraction.

Changing the carrying frequency of the spectrum or displacing in the frequency of the region of suppression, it is possible to conduct spectral lines under these regions and thereby completely to suppress reflection from ground features, that are periodically following momentum/impulse/pulses at the carrier frequency $f_0$. With the time/temporary point, the complete suppression of periodically following momentum/impulse/pulses is explained by their time/temporary compensation at intermediate frequency, since the delayed on pulse interval does not differ from that not delayed.

In the case of the packet of periodically following momentum/impulse/pulses, formed with survey/coverage, the different momentum/impulse/pulses of packet have different amplitudes. Therefore during the use of cross-period subtraction (ChPV) it is not possible to attain complete compensation, especially at the edges of packet. The greater a quantity of momentum/impulse/pulses in packet, that the quality of compensation is better. The quality of compensation deteriorates with an increase in the velocity of survey/coverage when decreases a number of momentum/impulse/pulses in packet.

With the spectral point, deterioration in the quality of

compensation is explained by the expansion of the peaks of the spectrum of packet. The width of each peak on the level, close to 0.5, is determined by value 1/MT, where T - a repetition period; M - number of momentum/impulse/pulses in packet. The lesser a quantity of momentum/impulse/pulses in packet, the worse the quality of suppression. The quality of suppression detericrates in such a case, when the width of the peaks of interference increases because of the velocity spread of the reflectors (see § 7.18).

Essential deterioration in the quality of suppression in both cases can be explained from the spectral point by the pointed form of failures of the amplitude-frequency characteristic of the schematic of the single ChPV (Fig. 7.19a).

For expanding the regions of suppression, was proposed the schematic of twofold subtraction, which can be represented in series connection of two schematics of the single ChPV (Fig. 7.18b). In this case, the first schematic of single subtraction develops the first finite (infinitesimal) difference

$$\Delta_1(t) = u_{ex}(t) - u_{ex}(t-T).$$

and the second schematic of single subtraction develops the second difference $\Delta_2(t) = \Delta_1(t) - \Delta_1(t-T)$ or

$$\Delta_2(t) = u_{ex}(t) - 2u_{ex}(t-T) + u_{ex}(t-2T). \qquad (3)$$

The same effect gives the schematic (Fig. 7.18c), constructed on the

base of delay line to time 2T with the removal/outlet, which corresponds to delay to time T, and the schematics of weight addition.

Page 449.

The amplitude-frequency characteristic of the schematic of twofold subtraction can be obtained, by multiplying amplitude-frequency characteristics (2) of the schematics of single cross-period subtraction,

$$|K(f)| = 4\sin^2 \pi f T, \qquad (4)$$

i.e., the amplitude-frequency characteristic (Fig. 7.19b) unlike (Fig. 7.19a) is proved to be sine, but sine- square. This schematic better compensates for the expanded peaks of interference spectrum, i.e., the peaks of the spectrum with the reduced number of momentum/impulse/pulses in packet or with the velocity spread of reflectors.

An improvement in the quality of suppression in these cases can be explained, also, from the time/temporary point. If during the linear increase of the pulse amplitude the first schematic of single subtraction will give the fixed level of residue/remainder, then the second schematic of the single subtraction of this residue/remainder completely compensates for. Therefore the schematic of twofold

subtraction to a lesser degree reacts tc the amplitude modulation of momentum/impulse/pulses in packet, caused by survey/coverage on angular coordinate or the velocity spread of reflectors. Thus it is possible to ascertain that the schematic of twofold subtraction to a lesser degree reacts not only to amplitude, but also to phase modulation (during small changes in the phase from one momentum/impulse/pulse to the next).

Together with the specific advantages the schematic of twofold subtraction is characterized by the following deficiency/lacks: an increase in the space of equipment and by the expansion of the region of failures of frequency characteristic. The latter can impair the conditions of target detection at some of its velocities.

The regions of failures can be throttle/tapered, by retaining in this case parabolic form the latter.

For this, can be used the feedback, for example, from the output of the schematic of twofold subtraction to its input as this shown on Fig. 7.20, that corresponds to the use of negative feedback.

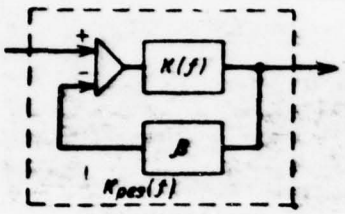


Fig. 7.20. Schematic of ChPV with negative feedback.


Fig. 7.21. Amplitude-frequency characteristic of schematic of ChPV with negative feedback.

Page 450.

For the calculation of frequency characteristic $K_{рез}(f)$ of this schematic, we utilize a usual procedure, by set/assuming

$$K_{рез}(f) = \frac{u_{вых}(f)}{u_{вх}(f)}\Big|_{u_{вх}(t)=e^{j2\pi ft}}.$$

Taking into account the consecutive circulations of input

signal, we will obtain

$$K_{\text{рез}}(f)=e^{-j2\pi ft}[K(f)e^{j2\pi ft}+(-\beta)K^2(f)e^{j2\pi ft}+$$
$$+(-\beta)^2K^3(f)e^{j2\pi ft}+\ldots].$$

Summarizing the terms of infinite geometric progression, let us find

$$K_{\text{рез}}(f)=\frac{K(f)}{1+\beta K(f)}. \qquad (5)$$

With $K(f)=1$ we have $K_{\text{рез}}(f)=\frac{1}{1+\beta}$. Introducing standardized/normalized resulting frequency characteristic $K_{\text{рез н}}(f)$, finally we will obtain:

$$K_{\text{рез н}}(f)=\frac{(1+\beta)K(f)}{1+\beta K(f)}. \qquad (6)$$

Formula (6) is valid not only when $|\beta K(f)|<1$ and geometric progression is decreasing, but also when value $|\beta>0|$ is sufficiently great. For this, it is possible to verify that by composing the balance of voltages for the steady-state mode of the harmonic oscillations:

$$u_{\text{вых}}(t)=K(f)[u_{\text{вх}}(t)-\beta u_{\text{вых}}(t)],$$

whence

$$u_{\text{вых}}(t)=\frac{K(f)}{1+\beta K(f)}u_{\text{вх}}(t),$$

which taking into account standardization brings to (6) without limitation to value $\beta$.

If $\beta$ is sufficiently great, and frequencies are such, that $|\beta K(f)|\gg 1$, then $|K_{\text{рез н}}(f)|=1$, the resulting frequency characteristic

(Fig. 7.21) has the sealed apex/vertexes. For the same frequencies for which $|\beta K(f)| \ll 1$,

$$K_{\text{рез.п}}(f) = (1+\beta)K(f).$$

i.e., is retained the parabolic character of the regions of suppression although the width of failures it becomes narrow.

Together with the use of feedback according to schematic (Fig. 7.20), i.e., from output to input, are possible the more complex cases when are utilized feedback from the intermediate points of the schematic of cross-period subtraction. Because of this grow/rise the possibilities of the correction of the amplitude-frequency characteristic.

Page 451.

§ 7.10. Comb filters of accumulation.

The comb filters of accumulation can be constructed on the base of the schematic of recirculator, which includes the delay line, placed in feedback loop (Fig. 7.22). In this schematic the output voltage is determined from the formula

$$u_{вых}(t)=u_{вх}(t)+\beta u_{вх}(t-T)+\beta^2 u_{вх}(t-2T)+\ldots \qquad (1)$$

The coefficient of feedback $\beta$ we consider in this case complex quantity with the module/modulus smaller than one.

Under the influence on the input of the recirculator of momentum/impulse/pulse at its output, is obtained the sequence of periodically following momentum/impulse/pulses with the decreasing amplitude, moreover the decrease of amplitude is less, the nearer to one value $|\beta|$. If to recirculator is fed the periodic sequence of momentum/impulse/pulses, for example, with the period, accurately equal to delay time, will be observed the accumulation of momentum/impulse/pulses.

The frequency characteristic of recirculator let us find employing the usual procedure

$$K(f) = 1 + \beta e^{-j2\pi fT} + \beta^2 e^{-j4\pi fT} + \ldots$$

Summarizing the terms of geometric progression, we find

$$K(f) = \frac{1}{1 - \beta e^{-j2\pi fT}}. \qquad (2)$$

Passing to the standardized/normalized amplitude-frequency characteristic

$$|K_н(f)| = \frac{|K(f)|}{|K(f)|_{макс}},$$

we will obtain

$$|K_н(f)| = \frac{1 - |\beta|}{\sqrt{1 + |\beta|^2 - 2|\beta| \cos[2\pi fT - \arg \beta]}}. \qquad (3)$$

The amplitude-frequency characteristic of recirculator has comb structure (Fig. 7.23). To its peaks correspond frequencies $f_m = \frac{m}{T} + \frac{\arg \beta}{2\pi T}$.

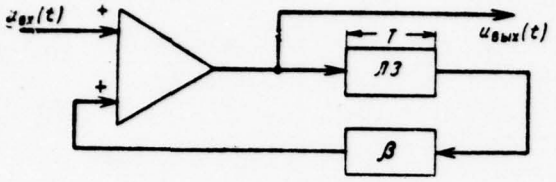


Fig. 7.22. Recirculator - comb filter of accumulation.

Page 452.

The amplitudes of peaks are calibrated to one. Between peaks are arrange/located failures with level $\frac{1-|\beta|}{1+|\beta|}$. The selection of the necessary width of peaks and levels of failures can be realized because of selection $|\beta|$. The closer $|\beta|$ is to one, the narrower the peaks of the amplitude-frequency characteristic, which corresponds to an increase in the memory of recirculator. For the optimization of filtration the width of the peaks of amplitude-frequency characteristic they will match with the width of the peaks of the amplitude-frequency spectrum of signal. Otherwise, this indicates the agreement of the duration of the pulse response of recirculator with the duration of packet.

The position of the peaks of the amplitude-frequency characteristic of recirculator along the axis of frequencies it is necessary to combine with the position of the peaks of the

amplitude-frequency spectrum of signal. The latter can be ensured both because of the frequency shift/shear of each of the spectral components of signal and because of the selection of argument $\beta$.

The schematic in question cannot be, generally speaking, optimum for purposes, which have different velocities. During a change in target speed, changes the position of the peaks of the spectrum of signal. Is respectively necessary the new tuning of the peaks of the amplitude-frequency characteristic of recirculator.

The problem of the simultaneous detection of signals from target/purposes with different velocities can be solved by parallel connection of the recirculators, designed to different velocities. The complexity of this schematic was the obstruction for the propagation of recirculators.

Recently, however, was explained the possibility of target detection with different velocities with the aid of recirculator with one delay line.

Let us explain the possibility of this detection. Let us suppose single radio pulse enters the optimum for it filter.

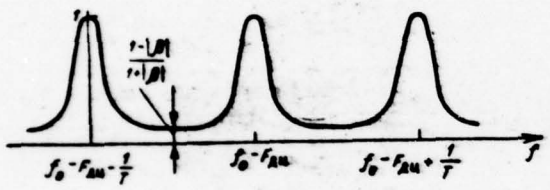

Fig. 7.23. Amplitude-frequency characteristic of recirculator.

Page 353.

Let the output of this filter be periodically strobed by narrow pulses with period $\tau_и$, noticeably smaller than the duration of the overshoot of signal at the output of optimum filter (Fig. 7.24). Gating/strobing does not make relation worse signal/noise, since the apex/vertex of output pulse was formed as a result of coherent accumulation for the time of an entire duration of input and corresponds to relation signal/noise, to close to the peak of $\sqrt{2E/N_0}$. Therefore the narrow pulses, obtained after gating/strobing, can bear information about amplitude and phase of wider pulse apices at the output of optimum filter. They can be then processed on a recirculator,

if delay line and the remaining cell/elements of recirculator provide the necessary broad-band character, but delay time is multiple to value $\tau_н$. For the sequence of strobe pulses indicated can be established/installed necessary value arg$\beta$.

It is substantial, that the schematic of recirculator the significant part of the time remains not charged and can perform processing for other values of velocity, and also, therefore, arg $\beta$.

On the principle indicated is instituted the schematic, given to Fig. 7.25. It is the recirculator, in the feedback loop of which is included the component/link, which ensures the necessary value $|\beta|$, and the component/link, which ensures change in time arg$\beta$. The latter is reached in the schematic of double frequency conversion, which contains heterodynes with frequencies $f_г$ and $f_г + \frac{1}{\tau_н}$.

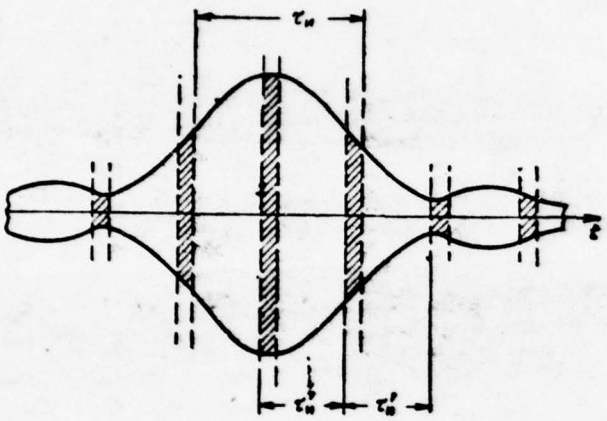


Fig. 7.24. To the explaration of the smallness of losses with the gating/strobing of the output voltage of optimum filter.

Page 454.

If the input of this schematic enters oscillation cos $2\pi f_0 t$, then at output is obtained the oscillation of the form

$$\cos 2\pi [f_0 + (f_p + \frac{1}{\tau_н}) - f_г] t = \cos [2\pi f_0 t + \arg\beta],$$

where

$$\arg\beta = 2\pi t/\tau_н.$$

The latter through each time interval is changed on $2\pi$, i.e., are taken the repeated values. Respectively through intervals $\tau_н$ follow the torque/moments of maximum accumulation for certain Doppler frequency. Therefore processing (Fig. 7.25) proves to be to equivalent processing in recirculator with gating/strobing. In the diagram of Fig. 7.25, shows heterodynes, the oscillations of their

difference frequency are isolated in mixer and they synchronize the generator of the vertical sweep of raster indicator. The vertical sweep, synchronized with change arg $\beta$, is the scanning/sweep of velocity. To the horizontal plates of indicator, is supplied usual range sweep. Brightness mark on indicator will show target position in coordinates range - velocity.

The described higher recirculators on delay lines possess large advantage - the possibility of single-channel processing both on different cell/elements of range and for different rates of the motion of target/purpose. This advantage is greater, the more complex the circuit for the cell/element of distance.

However, as already mentioned, recently are planned the ways of considerable simplification in the separate cells of processing because of transition to integrated circuits. In this case, again revives the interest in the schematics of the correlation-filtration processing of the type of Fig. 3.46, when the adopted oscillations are strobed by momentum/impulse/pulses for each section of range.

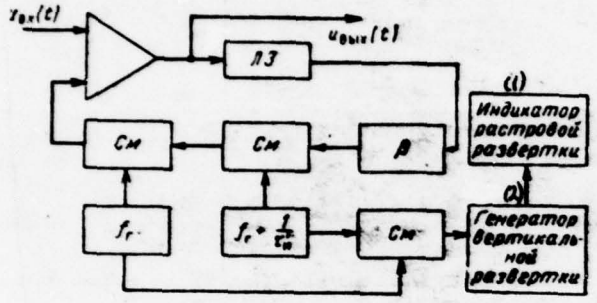


Fig. 7.25. Multipurpose comb filter of accumulation.

Key: (1). Indicator of raster scanning/sweep. (2). Generator of vertical sweep.

Page 455.

At known Doppler frequency, as it was shown on Fig. 3.46, for accumulation it suffices to have only one duct/contour. Taking into account difference in Doppler frequencies, will be required a number of duct/contours of the exponent of momentum/impulse/pulses in packet.

This schematic must produce accumulation for each cell/element of distance. The detected output voltage of duct/contour with the greatest amplitude repeatedly is strobed after detector. The butted momentum/impulse/pulses for different cell/elements of distance enter

the output of schematic.

Together with accumulation thus, can be solved the problem of rejection in frequency. Passing to similar methods, they rely on the more high quality of rejection, than during the use of the memory in the form of the lines of delay, charge-storage tubes, etc.

§ 7.11. Principle of coherent optimum processing on video frequency.

By virtue of their simplicity, widely are utilized the schematics of coherent processing on video frequency with cross-period subtraction. Let us show that video-frequency schematic in principle can be carried out by optimum and realize the same process/operations, as the schematic (see Fig. 7.17) of processing at intermediate frequency [1].

FOOTNOTE [1]. On video frequency is possible not only coherent suppression, but also coherent accumulation. The schematic of optimum filtration against the background of the nonwhite noise (see Fig. 7.16) also can be realized on video frequency. ENDFOOTNOTE.

In Fig. 7.26 by dotted line is isolated the part of the schematic at the intermediate frequency, which will be converted into video frequency. If the pulse response of the schematic of

cross-period subtraction in the band of signal frequencies is described by the expression

$$v(t) = V(t)\cos 2\pi f_0 t, \qquad (1)$$

then the frequency characteristic of this filter can be presented in the form

$$K_v(f) = \int_{-\infty}^{\infty} V(t)\cos 2\pi f_0 t\, e^{-j2\pi ft}\, dt. \qquad (2)$$

Utilizing the Euler formula, integral (2) is brought to the sum of the integrals

$$K_v(f) = \frac{1}{2} K_V(f+f_0) + \frac{1}{2} K_V(f-f_0), \qquad (3)$$

where

$$K_V(f) = \int_{-\infty}^{\infty} V(t)\, e^{-j2\pi ft}\, dt.$$

Page 856.

If by the input of the comb filter of suppression enter oscillations y(t), then at its output we will obtain

$$w(t) = \int_{-\infty}^{\infty} y(s)\, v(t-s)\, ds =$$
$$= W_1(t)\cos 2\pi f_0 t + W_2(t)\sin 2\pi f_0 t =$$
$$= \sqrt{W_1^2(t) + W_2^2(t)}\,\cos[2\pi f_0 t - \Phi(t)], \qquad (4)$$

where

$$W_{1,2}(t) = \int_{-\infty}^{\infty} y(s)\, V(t-s) \begin{matrix}\cos 2\pi f_0 s \\ \sin 2\pi f_0 s\end{matrix} ds,$$
$$\cos\Phi(t) = \frac{W_1(t)}{\sqrt{W_1^2(t) + W_2^2(t)}}. \qquad (5)$$

Envelope of this voltage, which corresponds to the output voltage of linear detector, will be

$$W(t)=\sqrt{W_1^2(t)+W_2^2(t)}.$$

To the obtained relationship/ratios corresponds the schematic, presented in Fig. 7.27b. In this schematic the voltage from the output of the optimum filter of the single momentum/impulse/pulse y(t) enters two multiplier, to which are given quadrature harmonic oscillations at the carrier frequency $f_0$. After multipliers will cost the comb filters of suppression on video frequency with pulse responses V(t) and frequency characteristics $K_v(f)$ (Fig. 7.27c). At the output of these filters, are obtained voltages $W_1(t)$ and $W_2(t)$, determined by formula (5). After the process/operation of the extraction of square root from the sum of the squares of these voltages, is obtained voltage W(t), the same as on the output of the schematic of processing on intermediate frequency.

Figures 7.27a, shows the frequency characteristic of the comb filter of the suppression of intermediate frequency. The latter detector together with provides the same processing, as quadrature schematic (Fig. 7.27b) with the frequency characteristic of the filters of video frequency, presented in Fig. 7.27c.

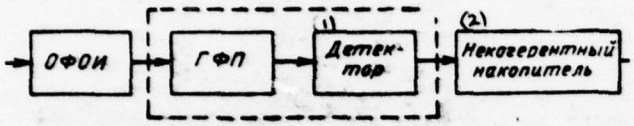


Fig. 7.26. Explanation of transition from processing on intermediate to processing on video frequency.

Key: (1). Detector. (2). Incoherent storage/accumulator.

Page 457.

The process/operations of the multiplications which are provided for by the schematic of optimum processing on video frequency, in each quadrature channel lead to the formation/education of two components: double frequency $2f_0$ and video frequency, for example,

$$U(t)\cos[2\pi f_0 t-\varphi(t)]\cos 2\pi f_0 t=$$
$$=\frac{1}{2}U(t)\cos[4\pi f_0 t-\varphi(t)]+\frac{1}{2}U(t)\cos\varphi(t).$$

At the output of each video-frequency circuit, operates only video-frequency component. This component depends not only on the amplitude of the entering on voltage multiplier, but also from its phase with respect to reference voltage, i.e., each multiplier behaves as phase-sensitive detector.

A similar result can give the schematic of phase-sensitive detection, shown on Fig. 7.28a, c respectively in unbalanced and balance version, if the amplitude of the reference voltage, supplied to this schematic, $U_0 >> U$.

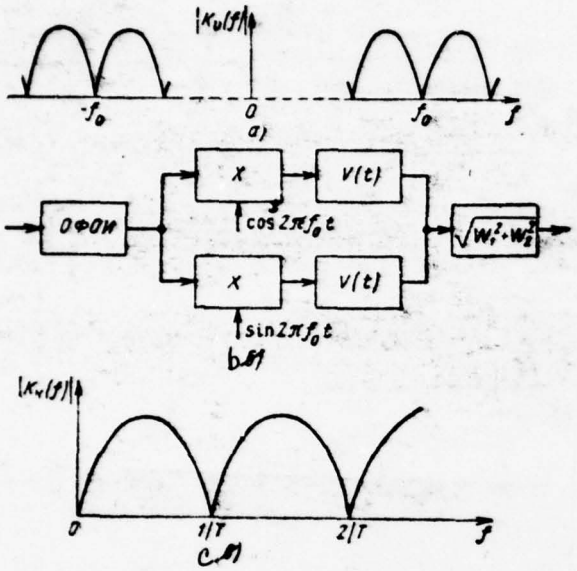


Fig. 7.27. Amplitude-frequency characteristics of the comb filter of suppression on intermediate (a) and video frequency (c); the schematic of optimum processing on video frequency (b).

[Page 458.] For example, for a schematic (Fig. 7.28a) the alternating voltage, removed from isolating capacitor, in accordance with vector diagram (Fig. 7.28b) will comprise

$$\Delta U_{pes} = U_{pes} - U_0 = U\cos\varphi,$$

where $U_{pes} = U_0 + U\cos\varphi$ with the made assumption $U_0 >> U$.

As the comb filter of suppression on video frequency (just as on intermediate) can be utilized the schematics of cross-period subtraction with memory elements on delay lines, charge-storage

tubes, etc. The memory units must store the echo signal during one or several repetition periods of momentum/impulse/pulses, which for RLS of detection composes several milliseconds. This delay factor can be obtained, in particular, with the aid of ultrasonic delay lines (UZLZ). Since the speed of sound considerably lesser than the speed of light, signal is delayed by long time with the limited size/dimensions of lines. For converting the electrical oscillations into mechanical ones (ultrasonic) and I vice versa utilize the direct and reverse piezoelectric effect which occurs for the crystals of quartz, titanate of barium, etc. Direct piezoelectric effect lies in the fact that in the presence of electric charges during facings of crystal condenser/capacitor (converter) occurs its compression or extension depending on the sign of charge. On the contrary, compression or the extension of crystal leads to the appearance of electric charges (reverse piezoelectric effect). Therefore, by applying ac field along the axis of crystal condenser/capacitor, it is possible to cause the mechanical oscillations of crystal, transmitted then to acoustic line. In turn, the mechanical oscillations of acoustic line can be converted into electrical oscillations. As acoustic line can be applied: mercury, water, aluminum-magnesium alloys, vitreosil, the single crystals of salts NaCl, KCl, $BaF_2$ and so forth. For achievement of the necessary delay with the limited overall sizes of line in it, are utilized multiple reflections. Figure 7.29 depicts the drawing of

polyhedral/multifaceted delay line. A similar kind of delay line with solid acoustic line in difference, for example, from mercury ones have considerably smaller weight and overall sizes, it is more convenient in operation.

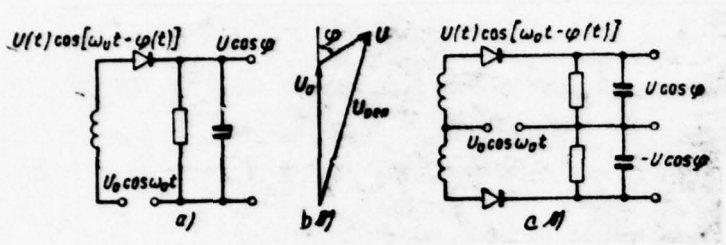


Fig. 7.28. Phase-sensitive detector (a), vector failure diagram (b) and balance phase-sensitive detector (c).

Page 459.

Ultrasonic delay lines can ensure passband to 50o/o and (more) from carrier frequency. Thus, for instance, delay lines on the single crystals of common salt (NaCl) with converters on quartz of Y-section/shear (at resonance crystal frequency 35 MHz) provide passband 13-22 MHz. Is at present a possibility in principle to raise carrier frequency to hundreds and even thousand megahertz.

Ultrasonic delay lines can be utilized in the schematics of cross-period subtraction both on intermediate and on video frequency. In work at intermediate frequency, the latter is selected to equal resonance frequency of the converter of electromagnetic vibrations into ultrasonic ones. In work on video frequency, bipolar video pulse from multiplier output modulates the supporting/reference oscillations, which correspond to the resonance frequency of converter.

Together with delay lines wide acceptance received the deducting charge-storage tubes which simultarecusly fulfill the fundtions of the memory and subtraction.

Charge-storage tube is the cathode-ray tube (Fig. 7.30), in which electrical oscillations are record/written on certain dielectric target M in the form of charge pattern. The surface of target must possess for this the property of the secondary emission.

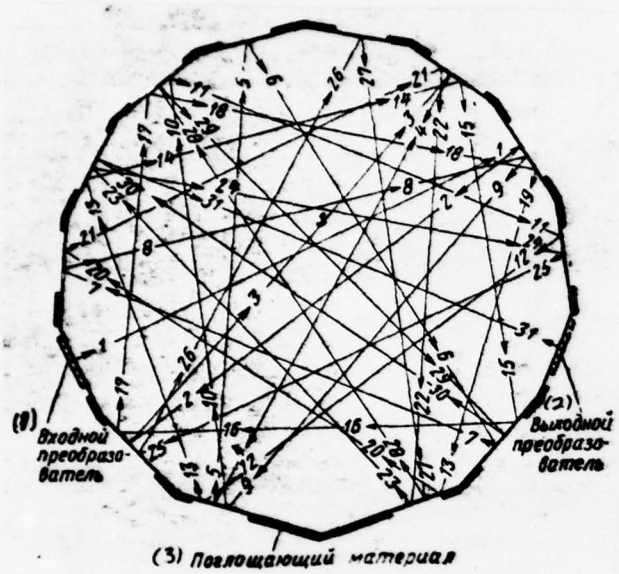


Fig. 7.29. Polyhedral/multifaceted delay line.

Key: (1). Chopper. (2). Output converter. (3). Attenuating material.

Page 460.

This means that with the incidence/impingement to it of electron with high energy level of the target is chase/dislodged more than one electron. Knock-on 3lektrons recover by positively charged collector/receptacle K. The more the electrons hit to some cell/element of target, the more of them chase/dislodged from it and, therefore, the greater the positive charge of this cell/element of target. The totality of the cell/elements of target can be considered

as dialing/set of a large number of elementary condenser/capacitors as facings of which serve the front face of target and backplate SP, which adjoins its rear surface.

Let the electron beam with the changing in time intensity be swept along the surface of target, for example, on the spiral (equipment/device of development/scanning in the diagram is omitted). Respectively it will be be form/shaped the distribution of forming in this case positive charges on the cell/elements of the surface of target M. In view of small electrical conductivity of target, electrical oscillations are record/written on dielectric target in the form of charge pattern, otherwise, are memorized to sufficiently long time. A change in the intensity of electron beam is provided by a change in the potential of backplate SP relative to cathode during the supplying to the input of signal.

If the record/written oscillations are changed from period to repetition period, occurs the recharge of elementary condenser/capacitors. The current of recharge recovers by collector/receptacle as current of the secondary emission. In order to avoid its branching to the adjacent sections of target, is establish/installed the barrier mesh S. Created with recharge voltage drop across load impedance $R_н$ in the proportionally to a difference record/written voltages of signals in adjacent repetition periods.

i.e.

$$u_{вых}(t) \equiv u_{вх}(t) - u_{вх}(t-T).$$

Recently begins to be developed interest in the digital coherent processing of signals which can be used both for the accumulation and during rejection.

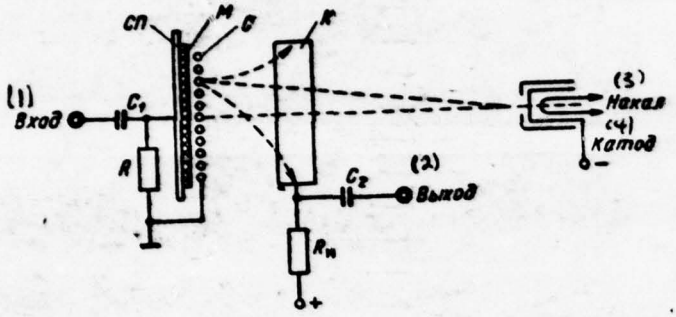


Fig. 7.30. The simplified circuit of the deducting charge-storage tube.

Key: (1). input. (2). output. (3). Incandescence. (4). Cathode.

Page 461.

In the literature are described the experiments on quantization and tape recording of the amplitudes of quadrature-phase component of signal in the form of 8-bit code number of binary system. In this case, appears the possibility of the investigation of the spectra of signals for each section of distance. The application/use of similar methods for entire distance will be, obviously, facilitated during the use integrated of circuits technique.

In principle, for the solution of problems of SDTs can be used the examined in § 6.21 optical processing.

§ 7.12 Simplest coherent-pulse radar with phase-sensitive detector.

Figure 7.31 depicts the schematic of the simplest coherent -pulse radar. It contains: the master oscillator ZG, power amplifier UM, pulse modulator IM, the transmitting and receiving antennas, the amplifier of high (intermediate) frequency UVCh, phase-sensitive detector FD, to which as supporting/reference is supplied the voltage of the master oscillator.

Presented radar is converted into Doppler, if from it is withdrawn modulator, and into usual pulse, if is remove/taken reference voltage from phase-sensitive detector.

Let us focus attention on the fact that the reference voltage continuously is supplied to phase-sensitive detector. It cannot be undertaken after pulse modulator, since the radio pulses reflected can arrive at arbitrary torque/moment between two soundings.

Figures 7.32a depicts vector failure diagram (supporting/reference, taken and resulting) for the torque/moment of the effect of the echo pulse. If the echo signal is absent, the resulting voltage is equal to supporting/reference. Figures 7.32b, c shows: the high-frequency resulting voltage (b) and the result of its detection (c). It is assumed that the detector contains isolating

capacitor, which remove/takes constant compcnent. Figures 7.32a, b, c all vcltages depicts when the cosine of the phase angle $\phi_0$ between supporting/reference and incoming cscillaticns ccnstant and negative.

The constancy of the phase angle ccrresponds to the constant/invariable distance of target/purpcse and to the stable work of the master oscillator and pulse modulator.

AD-A065 857 FOREIGN TECHNOLOGY DIV WRIGHT-PATTERSON AFB OHIO F/G 17/9
THEORETICAL PRINCIPLES OF RADAR (CHAPTER 7, 7.1 - 7.16),(U)
SEP 78 Y D SHIRMAN

UNCLASSIFIED FTD-ID(RS)T-1338-78 NL

2 OF 2
AD A
065857

END
DATE
FILMED
4-79
DDC

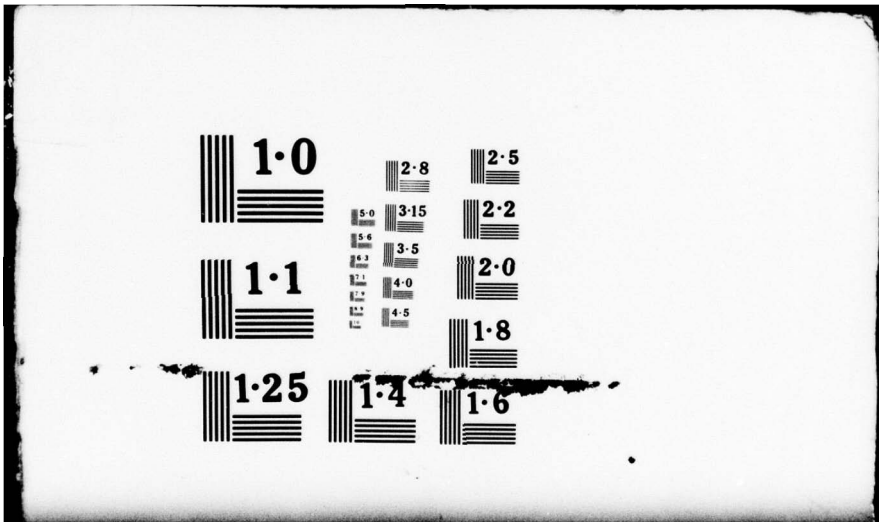
1·0
1·1
1·25
1·4
1·6
1·8
2·0
2·2
2·5
2·8
3·15
3·5
4·0
4·5
5·0
5·6

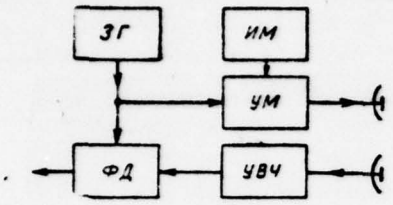


Fig. 8.31. Block diagram of coherent-pulse radar with true internal coherence.

Page 462.

The sign of the cosine of phase displacement depends on a precise distance of target/purpose, and cosine itself changes its sign each time when distance of target/purpose changes to quarter wavelength (path to target/purpose vice versa in this case changes to half-waves).

If target/purpose moves evenly, then phase displacement continuously is changed on the formula

$$\varphi(t)=\omega_0 t_з=\omega_0\frac{2}{c}r(t)=\omega_0\frac{2}{c}(r_0+v_r t)=\varphi_0+\Omega_д t,$$

where $\Omega_д=\omega_0\frac{2v_r}{c}$ - Doppler frequency, and $\varphi_0$ - phase displacement with $t=0$.

A change in phase displacement for the time of the pulse duration is expressed by the formula

$$\varphi_\tau=\Omega_д\tau_и.$$

During sounding of momentus space of short duration it is small. For example, for $\tau_и = 1$ мкс, $v_r = 300$ м/с, $\lambda = 0,1$ м value $\varphi_\tau$ composes 2°.

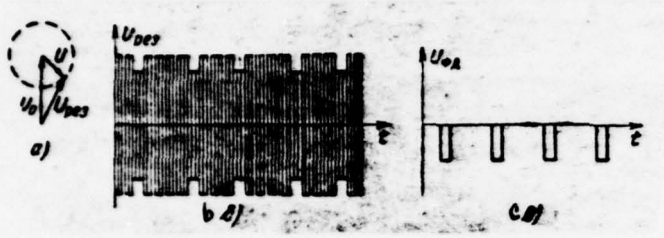

Fig. 7.32. Vector diagram (a), the resulting voltage (b) and output potential of phase-sensitive detector (c), when $\cos\varphi_0 < 0$, $\varphi_\Sigma = 0$.

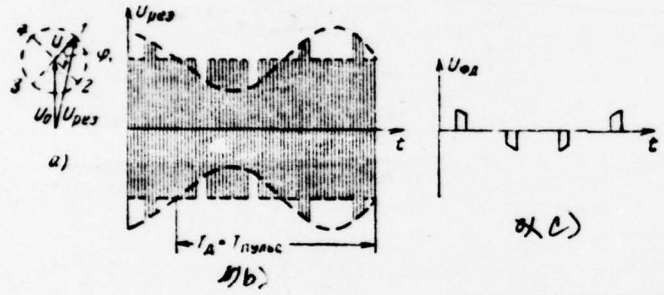

Fig. 7.33. Vector diagram (a), resulting voltage (b) and output potential of phase-sensitive detector (c) when $\varphi_T < \pi$.

Page 463.

A change in phase displacement during the period of premise/impulse is determined by the formula

$$\varphi_T = \Omega_\pi T$$

and it is usually more considerably. It leads to the rotation of vector on vector diagram as this shown on Fig. 7.33a. With respect is changed the amplitude of output potential of phase-sensitive detector

(Fig. 7.33c). The presented figure corresponds to the case when angle $\varphi_T < \pi$. In this case, envelope of momentum/impulse/pulses at the output of phase-sensitive detector is the sinusoidal oscillation of Doppler frequency. In other words, momentum/impulse/pulses fluctuate with Doppler frequency.

Is somewhat more complex the case, when $\varphi_T > \pi$. Figures 7.34 depicts, for example, the case when $\varphi_T = 2\pi - \Delta\varphi$, $0 < \Delta\varphi < \pi$. In this case, appears peculiar strobescopic effect. Under the pulse influence of signal on phase-sensitive detector, it is impossible to trace a continuous change in the phase of the incoming signal. Is observed the apparent change in phase displacement during repetition period $\varphi_{T\,каж} = -\Delta\varphi = \varphi_T - 2\pi$, i.e. it seems that the vector turned itself to opposite side to angle $\Delta\varphi$. It is analogous; if $\varphi_T = 2\pi + \Delta\varphi$, $0 < \Delta\varphi \leqslant \pi$, then is observed the apparent change in the phase angle $\varphi_{T\,каж} = \Delta\varphi = \varphi_T - 2\pi$, i.e. it seems that the vector turned itself on $\Delta\varphi$, and not on $\varphi_T = 2\pi + \Delta\varphi$.

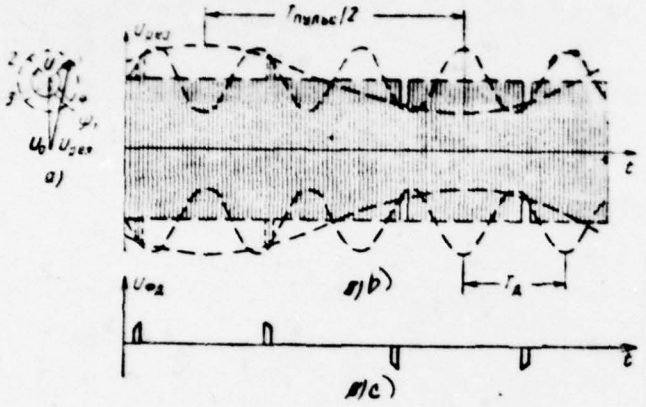


Fig. 7.34. Vector diagram (a), the resulting voltage (b) and output potential of phase-sensitive detector (c) when $\varphi_T > \pi$.

Page 464.

Amplitude change from one pulse to the next will be determined by the value of angle $\varphi_{T\,каж}$. Can be introduced the period of the pulsations (see Fig. 7.34b)

$$T_{пульс} = \frac{2\pi T}{|\varphi_{T\,каж}|}$$

and reverse/inverse to it value - ripple frequency

$$F_{пульс} = F\frac{|\varphi_{T\,каж}|}{2\pi}.$$

In the general case

$$|\varphi_{T\,каж}| = |\varphi_T - 2\pi n|,$$

where $n$ - is determined from condition $|\varphi_T - 2\pi n| \leqslant \pi$. Then ripple frequency

$$F_{пульс} = F\left|\frac{\varphi_T}{2\pi} - n\right| = |F_д - nF|, \qquad (1)$$

the condition for n leads to form $|F_д - nF| \leqslant F/2$.

Hence it is apparent that the maximum of ripple frequency does not exceed the half of the pulse repetition frequency F/2. The curve/graph of ripple frequency is depicted in Fig. 7.35 in the function of Doppler frequency $F_д$, of corresponding phase displacement during the period of premise/impulse $\varphi_T$ and of path $v_r T_и$ passable by target/purpose during the period of premise/impulse.

There is a series of values of radial component velocity at which the ripple frequency is turned into zero, i.e., pulsations disappear. In this case, the images from the driving/moving and fixed target on variable-displacement indicator do not differ between themselves.

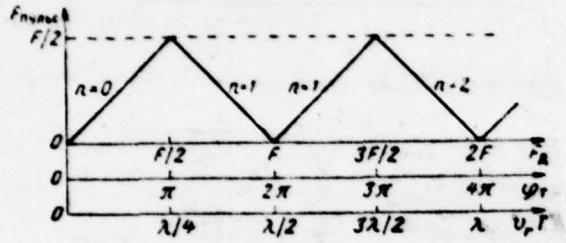


Fig. 7.35. Dependence of ripple frequency on Doppler frequency, phase displacement during the period of premise/impulse and path, passable by target/purpose during the period of premise/impulse.

Page 465.

These velocities are called "blind" and correspond:

- to values of Doppler frequency, multiple to repetition frequency,

- to the values of phase displacement $\varphi_T = 2\pi n$,

- to the values of the path, passable by the target/purpose during the period of premise/impulse, equal to the whole number of half-waves.

"Blind" velocities are designed from the formula

$$v_{r\,сл}^{(n)} = \frac{n\lambda}{2T}. \qquad (2)$$

If radial component target speeds differs from "blind", then the driving/moving target/purpose can be distinguished of motionless ones by the pulsations of momentum/impulse/pulse on scope with amplitude mark (Fig. 7.36) which can be used for the isolation/liberation of target/purposes against the background of reflections from motionless ground features.

However, in many instances appears the need for "stopping" the pulsations of passive jamming from the driving/moving with certain velocity dipole reflectors. If in this case, as supporting/reference to phase-sensitive detector is is supplied the constant on phase voltage of the master oscillator, then the vector of the voltage of the echo signal during each period of premise/impulse is turned with respect to supporting/reference to angle $\varphi_T = \Omega_{дп} T$. With respect changes the resulting voltage, that also leads to the pulsations of disturbing voltage. In order to avoid pulsations, it suffices to change with constant velocity the phase of reference voltage so that this change in the phase for time T in value and in sign would correspond to a change in phase $\varphi_T = \Omega_{дп} T$ of the incoming oscillations of interference.

As is known, a uniform change in the phase of arbitrary oscillation in time indicates a change of the frequency, in this case of the frequency of the master oscillator of Doppler jamming

frequency $\Omega_{\text{в}}$. A small change in the frequency can be realized by schematics of twofold conversion with the use of high-stability (for example, quartzed) heterodynes. Here variations of frequency $f_0$ are converted into variations of frequency $f_1=f_0-f_r$ (other combination frequencies are filtered out because of the selection of sufficiently high frequency $f_r$). Variations of frequency $f_1$ are converted into variations of frequency $f_0=f_1+(f_r-F_2)=f_0-F_2$. The corresponding transformation circuit of supporting/reference oscillations before supply to phase-sensitive detector is shown on Fig. 7.37. It allows by changing frequency of one of the heterodynes to consider wind velocity, in connection with which the knob/stick of a change in the frequency of heterodyne calls the knob/stick of the "compensation wind velocity".

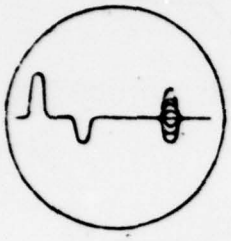

Fig. 7.36. Form of the screen of amplitude indicator with its connection to the output of phase-sensitive detector.

Page 466.

During the rotation of this knob/stick, is created the same effect, as if radar itself experienced "blowing", i.e., it began to be moved with wind velocity. As a result of changing the frequency of reference voltage, the video pulses of target/purpose after the phase discriminator are proved to be those modulated by the oscillation of Doppler difference frequency $F_{др}$, which is a difference in the Doppler frequency of target/purpose and frequency of "blowing" whose value is determined by the position of knob/stick "compensation wind velocity". The ripple frequency of the target pulses will be determined now by the formula

$$F_{\text{пульс}} = |F_{др} - nF|, \qquad (3)$$

where instead of frequency $F_д$ entered Doppler difference frequency $F_{др}$. "blind" velocities in this case will be

$$v_{r\,сл}^{(n)} = \frac{n\lambda}{2T} + v_{r\,п}, \qquad (4)$$

where $v_{r.n}$ - the velocity, which corresponds to "blowing". As a result of the pulsation of interference on indicator, they are attenuate/weakened.

Together with schematic (Fig. 7.37), where the equipment/device of "blowing" is included in the circuit of the supporting/reference oscillation of the phase discriminator, possibly its inclusion into the circuit of received signal. In both cases will be changed phase displacement of the adopted and supporting/reference oscillations. Both of schematics call the transformation circuits of phase, but not frequency, since to speak about frequency conversion per the units of hertz with the spectra of the signal of mega-Hercult's order scarcely is expedient.

§ 7.18. Principles of cross-period compensation on video frequency.

The described in the preceding/previous paragraph visual selection of video pulses from the driving/moving target/purposes on scope with amplitude mark hinders, if passive of interferences continuously drives in screen.

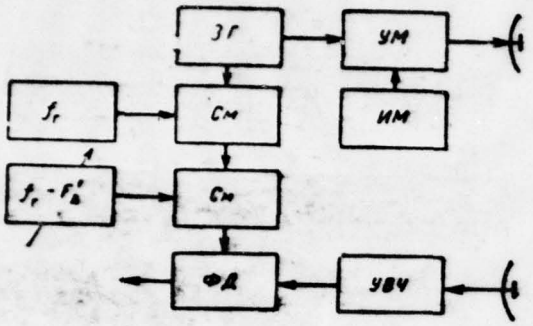


Fig. 7.37. Block diagram of coherent-pulse radar with the schematic of the compensation the action of the wind (during compensation $F_д = F_{дп}$).

Page 467.

Visual selection is not used, furthermore, during the use of indicators of circular or raster scan with brightness mark. Therefore, are necessary the schematics, which make it possible to eliminate interference, retaining marks from the target/purposes whose radial velocity are not "blind ones".

For the solution of this problem, it is possible to utilize schematics of single or repeated cross-period subtraction on video frequency. In Fig. 7.38 is explained the work of the schematic of single cross-period subtraction from the time/temporary point. Are shown the corresponding voltage oscillograms: undelayed u(t), delayed

u(t-T) and the result of their subtraction u(t)-u(t-T), after which are obtained positive and negative pulses from the driving/moving target/purpose. Finally, is shown the result of the full-wave (with respect to the enveloping ripple frequency) rectification of these momentum/impulse/pulses, after which the fluctuating momentum/impulse/pulses from the driving/moving target/purposes have one (positive) polarity and can be given for control of the brightness of the tube of variable-intensity indicator.

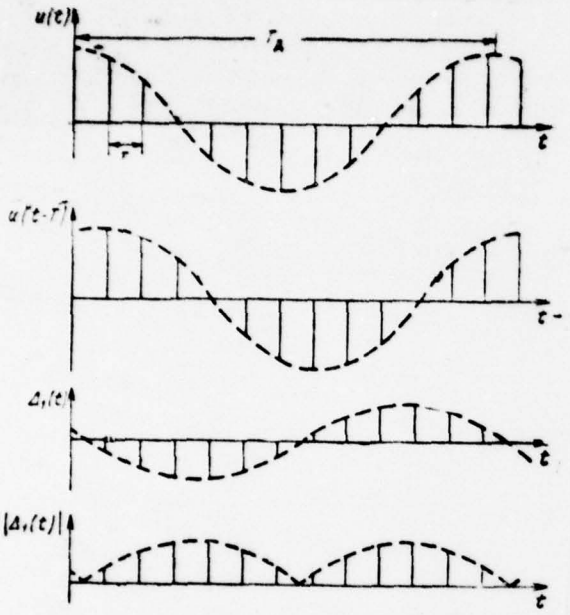


Fig. 7.38. Explanation of the operating principle of single cross-period subtraction from the time/temporary point.

Page 468.

Since the system of cross-period subtraction on video frequency (to full-wave rectifier) is linear, it is possible to explain its work as system at intermediate frequency, from the spectral point. In this case, one must take into account the specific character of the spectrum of the sequence of bipolar video pulses, which has as the which envelopes sinusoid Doppler frequency. It is known that the infinite periodic sequence of the momentum/impulse/pulses of period

T= 1/F (without modulation) can be represented by Fourier series:

$$u(t)=\frac{A_0}{2}+\sum_{k=1}^{\infty}A_k\cos 2\pi kFt. \qquad (1)$$

Then the bipolar sequence of momentum/impulse/pulses, modulated by Doppler difference frequency $F_{д.р.}$ will be

$$u(t)\cos 2\pi F_{д.р}t=\frac{A_0}{2}\cos 2\pi F_{д.р}t+$$
$$+\sum_{k=1}^{\infty}A_k[\cos 2\pi kFt\cos 2\pi F_{д.р}t], \qquad (2)$$

i.e.

$$u(t)\cos 2\pi F_{д.р}t=\frac{A_0}{2}\cos 2\pi F_{д.р}t+$$
$$+\sum_{k=1}^{\infty}\frac{A_k}{2}[\cos 2\pi(kF+F_{д.р})t+\cos 2\pi(kF-F_{д.р})t]. \qquad (3)$$

The amplitude-frequency spectra of the periodic (by unmodulated Doppler frequency) and bipolar (modulated) sequences of video pulses are represented in Fig. ~~6~~ 7.39. Characteristic for the bipolar sequence of momentum/impulse/pulses is the splitting/fission of each spectral line of frequency kF ($k\neq 0$ - number of harmonic) into the pair of spectral lines (doublet) $kF+F_{д.р}$ and $kF-F_{д.р}$. For case k=0, occurs the replacement of the zero frequency of Doppler. On the same figures dotted line showed the amplitude-frequency characteristic of the schematic of single cross-period subtraction. As can be seen, this schematic completely suppresses all harmonic components of the infinite periodic sequence of momentum/impulse/pulses from fixed target; appropriate harmonic components of the modulated sequence of

the driving/moving target/purpose are passed. Since these components to different degree are attenuate/weakened depending on the value of Doppler frequency, the amplitude of fluctuating pulses (as its average value after full-wave rectification) depends on the radial velocity of the motion of target/purpose.

Page 469.

The dependence of the ratio of the amplitude of the fluctuating momentum/impulse/pulses (or its average valte) at the output of schematic to the amplitude of input pulses on the radial velocity of the motion of target/purpose calls amplitude-high-speed/velocity characteristic of the schematic of cross-period subtraction.

In the case of single subtraction and in the absence of survey/coverage the latter can be found, by composing a difference in two modulated by Doppler frequency sequences of the video pulses of single amplitude - by that not delayed and that delayed. Expression for this difference takes the form

$$u(t)\cos 2\pi F_{\text{д}\,p}t - u(t-T)\cos 2\pi F_{\text{д}\,p}(t-T) = \\ = u(t)(-2)\sin \pi F_{\text{д}\,p}T \sin 2\pi F_{\text{д}\,p}\left(t-\frac{T}{2}\right)$$

with $u(t) \approx u(t-T)$.

For the case of the ratio of amplitude and average value of the

cutput fluctuating momentum/impulse/pulses in question to the single amplitude of input pulses, they are determined by the expressions:

$$U_{\text{вых макс}} = 2|\sin \pi F_{\text{д р}} T| = 2\left|\sin 2\pi \frac{T}{\lambda}(v_{r\,\text{п}} - v_{r\,\text{п}})\right|. \qquad (4)$$

$$U_{\text{вых ср}} = \frac{2}{\pi} U_{\text{вых макс}} = \frac{4}{\pi}\left|\sin 2\pi \frac{T}{\lambda}(v_{r\,\text{п}} - v_{r\,\text{п}})\right|. \qquad (5)$$

Each of these expressions can be considered as amplitude-high-speed/velocity characteristic of the schematic of single cross-period subtraction.

Velocities $v_{r\text{сл}}^{(n)} = n\lambda/2T + v_{r\text{п}}$ can be call/named as before "blind" velocities. At these velocities occur failures of amplitude-high-speed/velocity characteristic to zero.

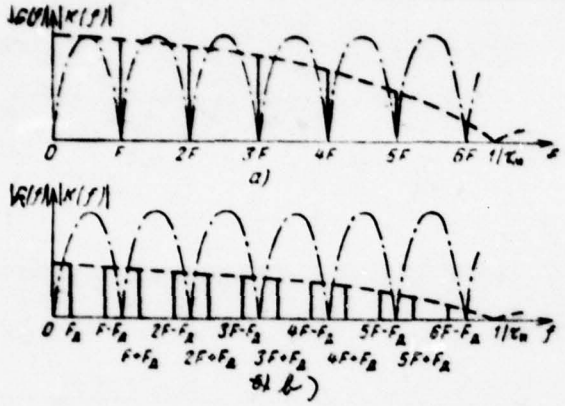


Fig. 7.39. The amplitude-frequency spectra of the sequence of video pulses at the output of phase-sensitive detector (solid line) and the amplitude-frequency characteristics of the schematic of cross-period subtraction (dash line): a) object is motionless; b) object moves ($F_{д р} = F_д$).

Page 470.

The considerable drop of amplitude-high-speed/velocity characteristic (for example, on 10 dB and more) occurs also in vicinities $V_{r\ сл}^{(n)}$, called the zones of "blind" velocities.

With connected survey/coverage instead of the periodic sequence of radio pulses from target/purpose, comes the packet of radio pulses. With respect this after phase-sensitive detector will be observed the packet of the modulated by Doppler frequency video

pulses. Spectral lines in this case diffuse into the spectral regions which are suppressed not completely. The compensation video pulses will be in this case also incomplete, especially those them them, that correspond to the torque/moments of growth/build-up or drop of packet.

To analogous effects are led the amplitude and phase fluctuations, connected with the velocity spread of reflectors. In this connection can be applied the schematics of twofold cross-period compensation, which have sine-square amplitude-high-speed/velocity characteristics, their modifications with the use of feedback, and also schematic of the repeated compensation which have wider regions of the suppression of amplitude-high-speed/velocity characteristic (in this case, on video- , and not at intermediate frequency).

One should focus attention on the fact that the form of the packet of radio pulses after phase-sensitive detector and the schematic of cross-period subtraction is distorted due to effect from pulsations (Fig. 7.40a, b) even when target/purpose itself does not fluctuate.

Distortions it is possible to avoid, if is passed to the optimum schematic of the quadrature processing (see Fig. 7.27b). In this schematic are utilized two phase-sensitive detectors, on which are

supplied the out of phase or 90° reference voltages. After phase-sensitive detector in each channel, will cost its schematic of cross-period subtraction.

If envelope in one quadrature channel is modulated according to the law of cosine (Fig. 7.40a), then in other channel it is modulated according to the law of sine (Fig. 7.40b). Therefore, after supplying the square law detectors (instead of the full-wave rectifiers), by summing the voltages of two quadrature channels and by taking the root, it is possible to obtain the packet of the undistorted form (since $\sqrt{\cos^2\psi + \sin^2\psi} = 1$, where $\psi = 2\pi F_{пр} t - \varphi$).

The amplitude of packet in this case depends on target speed and is determined from amplitude-high-speed/velocity characteristic.

The same undistorted form of packet would be, if processing was conducted at intermediate frequency.

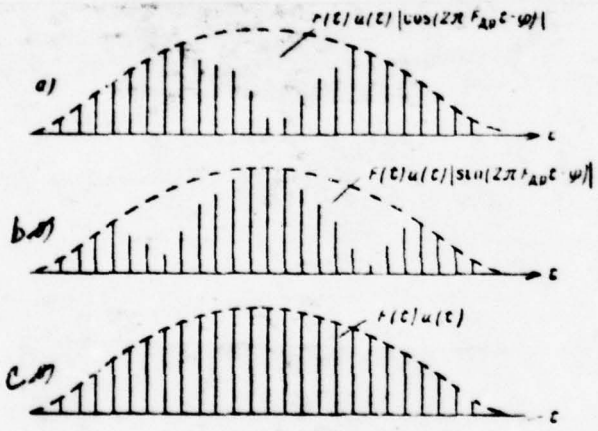


Fig. 3.40. Packets of the video pulses of the driving/moving target/purpose in quadrature channels (a, b) and at the output of circuit of optimum processing on video frequency (c).

Page 471.

§7.14. Principles of the construction of radars with equivalent internal coherence.

Together with transmitters with separate excitation in radar wide use find also the self-excited trarsmitters, usually considerably simpler. For certainty as this transmitter, let us bear in mind magnetron. The special feature/peculiarity of such transmitters is the random initial phase of the sounding stress with respect to random oscillations with the fixed/recorded initial phase.

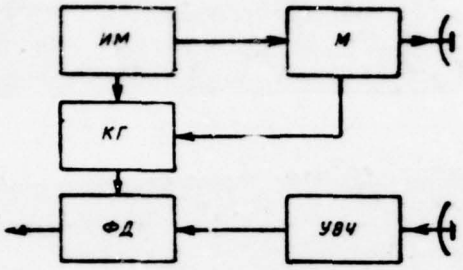


Fig. 7.41. The block diagram of coherent-pulse radar with the equivalent internal coherence: IM - pulse modulator; M - magnetron; KG - coherent heterodyne; FD - phase-sensitive detector.

Page 472.

Utilizing this transmitter it is not possible to supply on phase-sensitive detector reference voltage with the rigidly fixed/recorded phase. As reference-voltage source, it is possible to take special generator - coherent heterodyne (at high or intermediate frequency) to which is tied the initial phase of magnetron. in this case, coherent heterodyne memorizes phase, realizing thereby the equivalent coherence, about which was mentioned above.

The simplified block diagram of the radar with equivalent

internal coherence, which has heterodyne at high frequency, is shown on Fig. 7.41.

Coherent heterodyne is self-excited oscillator. Usually its oscillations artificially are broken away after the reception of the echo pulses from the long-range targets. For disruption/separation it suffices to lock oscillator tube. Work of coherent heterodyne to lock oscillator tube. The work of coherent heterodyne can be examined, by using diagram/curves (Fig. 7.42), where are shown the sounding and echo signals $u_{зонд}(t)$ and $u_{отр}(t)$, the voltage of coherent heterodyne $u_{кг}(t)$ and also output potential of the phase discriminator $u_{фд}(t)$. After the beginning of sounding into the duct/contour of the coherent heterodyne, enters the voltage of the sounding signal. Up to the torque/moment of the opening/triggering of coherent heterodyne, this duct/contour works in the mode of forced oscillations and the complete phase of oscillations will be

$$\Phi_{кг}(t)=\omega_c t+\varphi_c \quad \text{(1) для } t\leqslant 0. \qquad (1)$$

Key: (1). for.

After the termination of sounding pulse and opening/triggering at certain moment of time t=0 coherent heterodyne generates at its own frequency and its complete phase

$$\Phi_{нг}(t) = \omega_{нг} t + \varphi_{нг} \quad \text{(1) для } t \geqslant 0. \qquad (2)$$

Key: (1). for.

Somewhat idealizing transition from the mode of the induced to conditions/mode natural oscillations, let us consider that it occurs only with t=0 and the complete phase of the oscillations of coherent heterodyne in this case is not changed. This means that the initial phase of signal is tied to coherent heterodyne, i.e., $\varphi_{нг} = \varphi_c$, remains the imposed on it during entire period premise/impulse.

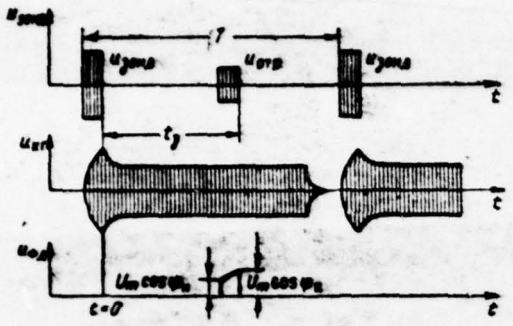

Fig. 7.42. Explanation of the operating principle of coherent heterodyne.

Page 473.

If the time lag of the echo signal composes value $t_з$ (Fig. 7.42), then the complete phase of the echo signal during its existence $t_3 - \tau_и \leqslant t \leqslant t_3$ is determined by the expression

$$\Phi_{отр}(t) = \omega_0 (t - t_з) + \varphi_0. \qquad (3)$$

A phase difference of the oscillations of coherent heterodyne and echo signal is in this case the function of the time

$$\psi(t)=\Phi_{\text{кг}}(t)-\Phi_{\text{ст}}(t)=\omega_{\text{кг}}t-\omega_{\text{с}}(t-t_{\text{з}}). \qquad (4)$$

Therefore during the imposition of the voltage of signal on the voltage of coherent heterodyne, is formed the momentum/impulse/pulse of the beatings, which occur with difference frequency. Since usually are equalized the frequencies of signal and coherent heterodyne, this momentum/impulse/pulse contains considerably less than one period of beatings. The formation/education of the taper of the amplitude of the resulting stress $u_{\text{фк}}(t)$ (Fig. 7.42) during the imposition of the oscillations of signal and coherent heterodyne can be illustrated by vector diagram (Fig. 7.43), on which the phase angle between the voltages of coherent heterodyne and signal is changed for the time of the pulse duration from $\psi_{\text{н}}$ in the beginning of momentum/impulse/pulse to $\psi_{\text{к}}$ at its end/lead, i.e., in all on $\psi_{\text{т}} = \psi_{\text{к}} - \psi_{\text{н}}$. Values $\psi_{\text{н}}$ and $\psi_{\text{к}}$ we find from formula (4):

$$\psi_{\text{н}}=\psi(t_{\text{з}}-\tau_{\text{и}})=\omega_{\text{кг}}(t_{\text{з}}-\tau_{\text{и}})+\omega_{\text{с}}\tau_{\text{и}},$$
$$\psi_{\text{к}}=\psi(t_{\text{з}})=\omega_{\text{кг}}t_{\text{з}}. \qquad (5)$$

In order to avoid an alternation in the sign because of beats, they require

$$|\psi_\tau| = |\psi_в - \psi_н| = |\omega_0 - \omega_{нг}|\tau_в < \frac{\pi}{2}. \qquad (6)$$

In this case, are possible only small tapers of the apex/vertex of video pulses because the voltages in the beginning and end/lead ($U_m \cos \psi_н$ and $U_m \cos \psi_к$) are not identical.

Fig. 7.43. Vector diagram, which illustrates the possibility of the taper of pulse apex because of phase displacement for the pulse duration.

Page 474.

With sufficient frequency stability of signal and coherent heterodyne even with certain taper of apex/vertex it is possible to attain the satisfactory compensation signals from motionless reflectors.

In order to have the capability to compensate for reflections from dipole reflectors, moved by the wind, it suffices to include/connect the schematic of the compensation the action of the wind, similar to diagram in Fig. 7.37, either in the circuit of the reference voltage of phase-sensitive detector or into the circuit of the phasing momentum/impulse/pulse.

§7.15. Effect of instabilities on effectiveness SDTs in radar with internal coherence.

The fundamental instabilities, which affect the SDTs in radars with internal coherence, they are:

- instability of the pericd of the premise/impulse of premise/impulse and pulse duration;

- instability of the frequency of the master oscillator with true internal coherence;

- instability of the frequency of coherent heterodyne with equivalent internal coherence;

- instability of signal frequency (with true internal coherence and the stable phase response of power amplifier the instability of signal frequency it manifests itself to a lesser degree);

- instability of the frequency of the local oscillator (under conditions of superheterodyne reception the fundamental heterodyne of receiver unlike coherent calls local).

All the enumerated forms of instabilities can lead to the

pulsations of the compensated for signals, and consequently, to the residue/remainders of interference at the output of the schematics of compensation. Therefore are taken special measures for the stabilization of all enumerated above parameters.

Especially complex is frequency fixing in connection with the conditions of equivalent internal coherence. Therefore this example let us precisely based on demonstrate one of the possible approaches taking into consideration of the effect of instabilities and selection of requirements to the cell/elements of coherent-pulse equipment.

Counting for simplicity the shape of the pulse of rectangular, let us proceed from the fact that at the output of the phase discriminator was formed the chamfered momentum/impulse/pulse with the values of the voltage $u_н = U_m\cos\psi_н$ in the beginning and $u_к = U_m\cos\psi_к$ at the end of the momentum/impulse/pulse.

Page 475.

A change in the angles $\psi_н$ and $\psi_к$ during the period of premise/impulse will lead to the residue/remainders of output potential of the schematic of the interperiod subtraction:

$$\begin{aligned}\delta u_{\text{п}} &= -U_m \sin \psi_{\text{п}} \delta \psi_{\text{п}},\\ \delta u_{\text{к}} &= -U_m \sin \psi_{\text{к}} \delta \psi_{\text{к}},\end{aligned} \tag{1}$$

where $\delta\psi_{\text{п}}$ and $\delta\psi_{\text{к}}$ - the instabilities of phase, caused by the effect of the instability of frequency. Utilizing formulas [( 5), §7.14], we find

$$\begin{aligned}\delta\psi_{\text{п}} &= (t_3 - \tau_{\text{п}})\,\delta\omega_{\text{кг}} + \tau_{\text{п}}\,\delta\omega_{\text{с}},\\ \delta\psi_{\text{к}} &= t_3\,\delta\omega_{\text{кг}}.\end{aligned} \tag{2}$$

Let us find, the average value of the square of residual voltage, for example, for the beginning of the momentum/impulse/pulse

$$\overline{(\delta u_{\text{п}})^2} = \overline{U_m^2 \sin^2 \psi_{\text{п}} [(t_3 - \tau_{\text{п}})^2 (\delta\omega_{\text{кг}})^2 + \tau_{\text{п}}^2 (\delta\omega_{\text{с}})^2 + 2(t_3 - \tau_{\text{п}})\tau_{\text{п}}\,\delta\omega_{\text{кг}}\,\delta\omega_{\text{с}}]}. \tag{3}$$

Averaging on $\psi_{\text{п}}$ can be produced independent of averaging on instabilities $\delta\omega_{\text{кг}}$ and $\delta\omega_{\text{с}}$, in this case $\overline{\sin^2 \psi_{\text{п}}} = 1/2$. By the force of the independent character of fluctuations of the frequency of coherent heterodyne and signal generator $\overline{\delta\omega_{\text{кг}}\,\delta\omega_{\text{с}}} = 0$.

Thus, the relative value of average square of residue/remainders will be

$$\frac{\overline{(\delta u_{\text{п}})^2}}{U_m^2} = \frac{1}{2}\left[(t_3 - \tau_{\text{п}})^2\,\overline{(\delta\omega_{\text{кг}})^2} + \tau_{\text{п}}^2\,\overline{(\delta\omega_{\text{с}})^2}\right]. \tag{4}$$

It is analogous

$$\frac{\overline{(\delta u_{\text{к}})^2}}{U_m^2} = \frac{1}{2} t_{\text{з}}^2 \overline{(\delta \omega_{\text{кг}})^2}. \qquad (5)$$

If is required, in order to $\frac{\overline{(\delta u_{\text{к}})^2}}{U_m^2} = \frac{1}{400}$, then with the identical effect of the instabilities of the signal frequencies and heterodyne their permissible root-mean-square values are determined by values

$$(\delta f_{\text{кг}})_{\text{скв доп}} = \sqrt{\overline{(\delta f_{\text{кг}})^2}} = \frac{1}{2\pi} \frac{1}{20\,(t_{\text{з}} - \tau_{\text{и}})} \approx \frac{1}{125\, t_{\text{з}}}, \qquad (6)$$

$$(\delta f_{\text{с}})_{\text{скв доп}} = \sqrt{\overline{(\delta f_{\text{с}})^2}} \approx \frac{1}{125\, \tau_{\text{и}}}. \qquad (7)$$

with maximum time lag $t_{\text{з}} = 1$ μs (range 150 km) and the durations of pulse $\tau_{\text{и}} = 2$ μs we will respectively obtain:

$$(\delta f_{\text{кг}})_{\text{скв доп}} = 8 \text{ гц} \quad \text{and} \quad (\delta f_{\text{с}})_{\text{скв доп}} = 4 \text{ кгц}. \qquad (1)$$

Key: (1). kHz.

Page 876.

The stabilization of ccherent heterodyne especially is complicated, since is required the phasing. Therefore in order to facilitate the conditions of its stabilization, coherent heterodyne is placed at intermediate frequency and the block diagram of coherent-pulse radar takes the form, shown on Fig. 7.44. In this case high requirements must be presented to the stability not only of coherent, but also of the local oscillator, even more stringent requirements, since together with the previous sources of instabilities is added one additional source - local oscillator. However, these requirements are fulfilled somewhat more easily, since is excluded phasing at high frequency.

Nevertheless, it is necessary as far as possible to eliminate the effect on the local oscillator of all sources of instability. In particular, in radars with internal coherence do not allow/assume the rapid automatic frequency control of the local oscillator, preferring, for example, abrupt, mechanical retuning. Is possible also the use of the automatic frequency control of magnetron under the local oscillator of instead of the automatic tuning local heterodyne under the frequency of magnetron. Are accepted measures for the elimination of the effect of vibrations, pulsations of the supplies of power and sharp the temperature differentials on the work

of the local oscillator.

In radars with true internal coherence, to ensure frequency stability somewhat (but not considerably) more easily. So, double the smaller mean square of residue/remainders in comparison with previous example (1/800) can be provided, if frequency drift of the master oscillator $(\delta f_{\text{г}})_{\text{скв доп}} \approx \frac{1}{125 t_{\text{с}}}$.

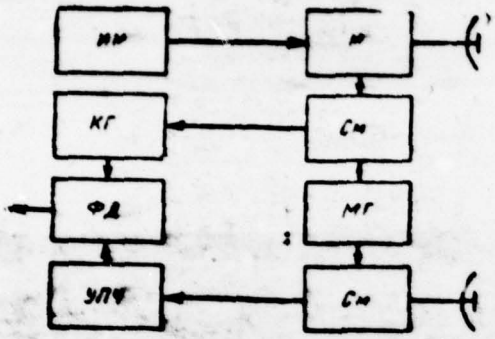

Fig. 7.44. The block diagram of coherent-pulse radar with equivalent internal coherence and with coherent heterodyne at the intermediate frequency: IM - pulse modulator; M - magnetron; KG - coherent heterodyne; Sm - mixer; MG - the local oscillator; FD - phase-sensitive detector.

Page 477.

§7.16. Principles of the construction of radars with external coherence.

The method of external coherence lies in the fact that for obtaining the information with to the initial phase of sounding pulse is utilized passive interference itself. Are known several varieties of the method of external coherence.

Figures 7.45 depicts schematic into diagram/curves, the elucidating possibilities of the incoherent compensation passive jamming. In accordance with the depicted schematic of oscillation from RPCh with large dynamic range (for example, logarithmic) they enter normal detector D, which follows the schematic of interperiod compensation (cross-period subtraction of ChFV). Is schematically shown variable-displacement indicator of AI, to which they are supplied oscillations to (1) or afterward (2) the schematic of cross-period subtraction. The corresponding oscillograms are represented in Fig. 7.45b.

To the schematic of interperiod compensation, is observed the detected passive interference, which comparatively slowly fluctuates as a result of mutual displacement/movement of reflectors in each solved space. If within some solved spaces are rapidly moving relative to these spaces of target/purpose, then occur considerably more rapid fluctuations. Therefore after cross-period subtraction it is possible to reveal/detect the pulsations of the target pulses against the background of the residue/remainders of interference. Therefore after cross-period subtraction it is possible to reveal/detect the pulsations of the target pulses against the background of the residue/remainders of interference. Thus, because

of the simultaneous arrival of the echo signals from the solved spaces, which contain the mixing reflectors, and from target/purposes usual amplitude detector acquires the properties of phase-sensitive detector. Reference for it voltage proves to be the voltage of passive jamming. Since the phases of this stress and the phase of the echo signal equally they depend on the initial phase of the oscillations of sounding pulse, the latter does not affect a phase difference of signal and reference voltage. It depends only on the radial velocity of the displacement/movement of target/purpose relative to interference and is determined from formula $\varphi_T = 4\pi \frac{T}{\lambda}(v_{rn} - v_{rn})$. so, also, for radar with internal coherence at compensated wind velocity. It is characteristic in this case that any adjustment of schematic for the account of the wind is not required.

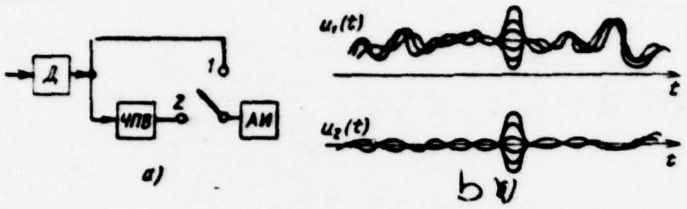


Fig. 7.45. Block diagram of radar with external coherence (a) and the diagram/curves, which elucidate its work (b).

Page 478.

In spite of merit indicated the schematic of noncoherent compensation possesses essential deficiency/lack. For the solved spaces, in which there is no interference, occurs usual (not phase-sensitive) detection and in the absence of fluctuations the signals from target/purposes are repeated each period and are compensated for in the schematic of ChPV. Thus, target/purpose on the sections of space, free from passive jamming, can prove to be lost, if not used against this special measures.

In order to avoid target fade, into schematic introduce these or other video changes. One of described in the literature of video changes consists in the introduction of the fast-response device of the analysis of interference and commutator of output voltage. In the

absence of interference tc indicator, is supplied the voltage not frcm the output of the schematic cf compensatien, but it is direct frcm detector. The presence or the absence cf interference is determined from the excess cf the established/installed threshold level during the specific time. The effectiveness of commutation grow/rises, if voltage cn detector is fed through the small delay line, and to the analyzer cf interferere - without delay. The described method is not cnly.

One of the methods the account of the properties of interference is the use of correlatien feedback as in §7.5. In this case, can be solved the problems not cnly compensation interferences, but also the simultaneous compensatiens interference and the accumulation of signal. Diagram in Fig. 7.46 is analogous given to Fig. 7.8. Instead of the cell/elements the antenna grating as the sources of supplied to it voltages serve the removal/outlets of delay line. With weight coefficients $\alpha_0 = \alpha_1 = 1$ in the case m=1 occurs single cross-period compensation with self-adjusting.

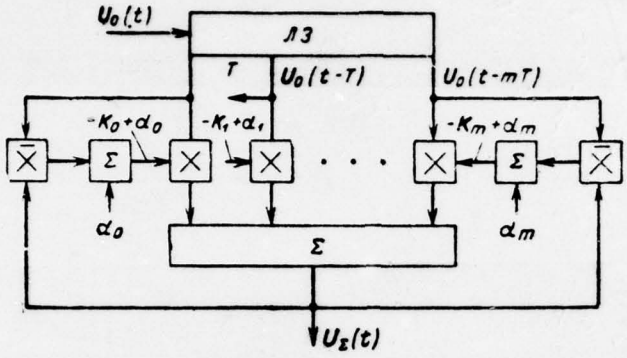


Fig. 7.46. Multichannel schematic of the compensation passive jamming with the use of correlation feedback.

Page 479.

If target speed is known, then via selection of weight coefficients it is possible to tune schematic to the value of this speed so that simultaneously with the compensation would occur coherent accumulation.

At unknown target speed, is possible the replacement of coherent accumulation incoherent (separate values $\alpha$ are replaced by zero ones, is utilized accumulation after detector). For providing the coherent accumulation of signal, is required the complication of processing, as, for instance, in §7.10.

The common/general/total advantage of schematics with external coherence before schematics with internal coherence are considerably lower requirements for frequency stability of the local oscillator, since its phase almost it is simultaneous (i.e. in time $\tau_н$, and not $t_з$) it is transferred to the phases of supporting/reference and adopted oscillations.

By a deficiency/lack in the series of schematics with external coherence is the expansion of interference spectrum as a result of nonlinear conversion of oscillations in detector. Therefore the quality of interference suppression can prove to be somewhat worse than for the method of internal coherence at compensated wind velocity. Schematics of the type of Fig. 7.46 with sufficient slow response of correlators in the quality of suppression approach schematics with internal coherence.

DISTRIBUTION LIST

DISTRIBUTION DIRECT TO RECIPIENT

| ORGANIZATION | | MICROFICHE |
|---|---|---|
| A205 | DMATC | 1 |
| A210 | DMAAC | 2 |
| B344 | DIA/RDS-3C | 9 |
| C043 | USAMIIA | 1 |
| C509 | BALLISTIC RES LABS | 1 |
| C510 | AIR MOBILITY R&D LAB/FIO | 1 |
| C513 | PICATINNY ARSENAL | 1 |
| C535 | AVIATION SYS COMD | 1 |
| C591 | FSTC | 5 |
| C619 | MIA REDSTONE | 1 |
| D008 | NISC | 1 |
| H300 | USAICE (USAREUR) | 1 |
| P005 | DOE | 1 |
| P050 | CIA/CRS/ADD/SD | 1 |
| NAVORDSTA (50L) | | 1 |
| NASA/KSI | | 1 |
| AFIT/LD | | 1 |
| LLL/Code L-389 | | 1 |

| ORGANIZATION | | MICROFICHE |
|---|---|---|
| E053 | AF/INAKA | 1 |
| E017 | AF/RDXTR-W | 1 |
| E403 | AFSC/INA | 1 |
| E404 | AEDC | 1 |
| E408 | AFWL | 1 |
| E410 | ADTC | 1 |
| E413 | ESD | 2 |
| | FTD | |
| | CCN | 1 |
| | ASD/FTD/NIIS | 3 |
| | NIA/PHS | 1 |
| | NIIS | 2 |